

Chulalongkorn University

## Chula Digital Collections

---

Chulalongkorn University Theses and Dissertations (Chula ETD)

---

2021

### Electrochemical tubular fixed-bed reactor for conversion of pressurized CO<sub>2</sub> to CO

Pakawat Sengchim

*Faculty of Engineering*

Follow this and additional works at: <https://digital.car.chula.ac.th/chulaetd>



Part of the [Chemical Engineering Commons](#)

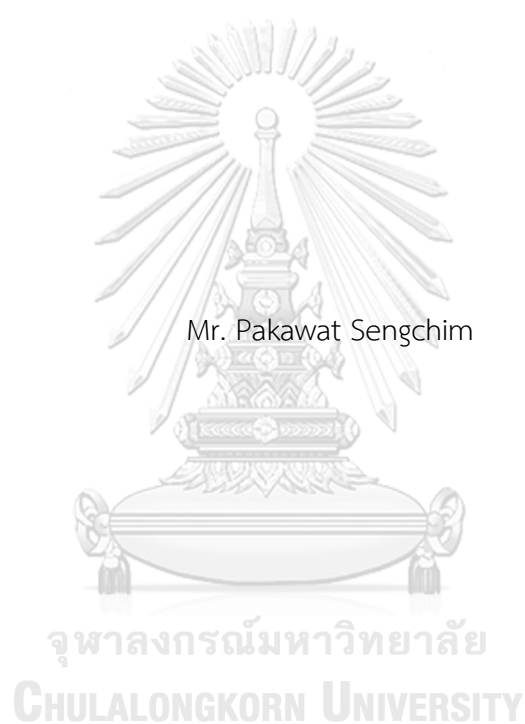
---

#### Recommended Citation

Sengchim, Pakawat, "Electrochemical tubular fixed-bed reactor for conversion of pressurized CO<sub>2</sub> to CO" (2021). *Chulalongkorn University Theses and Dissertations (Chula ETD)*. 4591.  
<https://digital.car.chula.ac.th/chulaetd/4591>

This Thesis is brought to you for free and open access by Chula Digital Collections. It has been accepted for inclusion in Chulalongkorn University Theses and Dissertations (Chula ETD) by an authorized administrator of Chula Digital Collections. For more information, please contact [ChulaDC@car.chula.ac.th](mailto:ChulaDC@car.chula.ac.th).

Electrochemical tubular fixed-bed reactor for conversion of pressurized CO<sub>2</sub> to CO



Mr. Pakawat Sengchim

A Thesis Submitted in Partial Fulfillment of the Requirements  
for the Degree of Master of Engineering in Chemical Engineering

Department of Chemical Engineering

FACULTY OF ENGINEERING

Chulalongkorn University

Academic Year 2021

Copyright of Chulalongkorn University

เครื่องปฏิกรณ์เคมีไฟฟ้าแบบท่อเบตนิ่งสำหรับการเปลี่ยนคาร์บอนไดออกไซด์ความดันสูงเป็น  
คาร์บอนมอนอกไซด์



วิทยานิพนธ์นี้เป็นส่วนหนึ่งของการศึกษาตามหลักสูตรปริญญาวิศวกรรมศาสตรมหาบัณฑิต  
สาขาวิชาวิศวกรรมเคมี ภาควิชาวิศวกรรมเคมี  
คณะวิศวกรรมศาสตร์ จุฬาลงกรณ์มหาวิทยาลัย  
ปีการศึกษา 2564  
ลิขสิทธิ์ของจุฬาลงกรณ์มหาวิทยาลัย

Thesis Title	Electrochemical tubular fixed-bed reactor for conversion of pressurized CO <sub>2</sub> to CO
By	Mr. Pakawat Sengchim
Field of Study	Chemical Engineering
Thesis Advisor	Assistant Professor PALANG BUMROONGSAKULSAWAT, Ph.D.

---

Accepted by the FACULTY OF ENGINEERING, Chulalongkorn University in  
Partial Fulfillment of the Requirement for the Master of Engineering

----- Dean of the FACULTY OF  
ENGINEERING  
(Professor SUPOT TEACHAVORASINSKUN, D.Eng.)

THESIS COMMITTEE

----- Chairman  
(Assistant Professor APINAN SOOTTITANTAWAT, Ph.D.)  
----- Thesis Advisor  
(Assistant Professor PALANG BUMROONGSAKULSAWAT, Ph.D.)  
----- Examiner  
(Assistant Professor RUNGTHIWA METHAAPANON, Ph.D.)  
----- External Examiner  
(Pongkarn Chakthranont, Ph.D.)

ภักวิวัฒน์ เชนงนิม : เครื่องปฏิกรณ์เคมีไฟฟ้าแบบท่อเบตนิ่งสำหรับการเปลี่ยน  
คาร์บอนไดออกไซด์ความดันสูงเป็นคาร์บอนมอนอกไซด์. ( Electrochemical tubular  
fixed-bed reactor for conversion of pressurized CO<sub>2</sub> to CO) อ.ที่ปรึกษาหลัก :  
ผศ. ดร.พลัง บำรุงสกุลสวัสดิ์

ปฏิกิริยาการลดคาร์บอนไดออกไซด์ถูกใช้ในการกระตุ้นการเปลี่ยนคาร์บอนไดออกไซด์  
เป็นคาร์บอนมอนอกไซด์ โดยปกติกระบวนการนี้จะศึกษาในสารละลายอิ่มตัวด้วย  
คาร์บอนไดออกไซด์ที่สถานะของเหลวโดยที่ความสามารถในการละลายของคาร์บอนไดออกไซด์ใน  
น้ำมีค่าที่ต่ำมาก (0.033 โมลาร์) ที่ความดัน 1 บาร์และที่อุณหภูมิห้อง ส่งผลต่ออัตราการ  
เกิดปฏิกิริยาและการถ่ายโอนมวล ในงานวิจัยนี้ได้ศึกษาเครื่องปฏิกรณ์เคมีไฟฟ้าแบบท่อเบตนิ่ง  
สำหรับปฏิกิริยาการเปลี่ยนคาร์บอนไดออกไซด์เป็นคาร์บอนมอนอกไซด์โดยมีการออกแบบจะ  
คำนึงถึงการขยายขนาดได้ง่ายและเครื่องปฏิกรณ์ประกอบด้วยเซลล์เคมีไฟฟ้าหลายเซลล์ที่สามารถ  
ต่อกันเป็นแบบอนุกรมได้ โดยแต่ละเซลล์ประกอบไปด้วย 3 ส่วนหลัก คือ แอโนด, อิเล็กโทรไลต์  
แข็ง และแคโทด นอกจากนี้โลหะซึ่งถูกนำมาใช้เป็นตัวเร่งปฏิกิริยาเคมีไฟฟ้าสำหรับการเปลี่ยน  
คาร์บอนไดออกไซด์เป็นคาร์บอนมอนอกไซด์ โดยที่มิน้ำไหลผ่านเซลล์เพื่อรักษาค่าการนำไฟฟ้า  
ของอิเล็กโทรไลต์และเพื่อรักษาปฏิกิริยาไฟฟ้าเคมี การศึกษาผลกระทบของความดัน อัตราการไหล  
และความต่างศักย์ที่ให้แก่ระบบที่มีผลต่ออัตราการเกิดปฏิกิริยาและผลผลิต จากการทดลองที่ความ  
ดัน 10 บาร์ อัตราการไหลที่ 60 มิลลิลิตรต่อนาทีและความต่างศักย์ 7 โวลต์ ค่าความเข้มข้นของ  
คาร์บอนมอนอกไซด์ได้ 1272 ส่วนในล้านส่วนและประสิทธิภาพของฟาราเดย์สูงที่สุดอยู่ที่ 19.61  
เปอร์เซ็นต์

จุฬาลงกรณ์มหาวิทยาลัย  
CHULALONGKORN UNIVERSITY

สาขาวิชา วิศวกรรมเคมี  
ปีการศึกษา 2564

ลายมือชื่อนิสิต .....

ลายมือชื่อ อ.ที่ปรึกษาหลัก .....

# # 6370219121 : MAJOR CHEMICAL ENGINEERING

KEYWORD: Electrochemical CO<sub>2</sub> reduction, Electrochemical tubular reactor, CO,  
Pressure

Pakawat Sengchim : Electrochemical tubular fixed-bed reactor for  
conversion of pressurized CO<sub>2</sub> to CO. Advisor: Asst. Prof. PALANG  
BUMROONGSAKULSAWAT, Ph.D.

Electrochemical CO<sub>2</sub> reduction reaction (CO<sub>2</sub>RR) can be used for activating the stable CO<sub>2</sub> molecule to the more active CO for downstream purposes. Usually, this process is carried out in CO<sub>2</sub>-saturated aqueous solutions. The low solubility of CO<sub>2</sub> in water of 0.033 M at 1 bar of CO<sub>2</sub> and room temperature hinders both kinetics and mass transfer. In this study, a novel electrochemical tubular reactor for electrochemical CO<sub>2</sub>RR is proposed. The design was made with ease of scale-up in mind. A reactor can contain multiple electrochemical cells connected in series. Each cell consists of 3 main parts: porous anode, porous solid electrolyte, and porous cathode, all of which allow bulk flow of gas streams through the tubular reactor. Zn is the active electrocatalyst at the cathode for the conversion of CO<sub>2</sub> to CO. Water is trickled through the cells to maintain electrolyte conductivity and also to sustain electrochemical reactions. The effects of CO<sub>2</sub> pressure and flow rate and applied voltage on the CO<sub>2</sub> conversion rate and yield are studied. About 1272 ppm of CO concentration and 19.61% of highest CO faradaic efficiency was obtained from a preliminary experiment conducted at 60 ml min<sup>-1</sup>, 7 V of CO<sub>2</sub> at 10 bar.

Field of Study: Chemical Engineering

Student's Signature .....

Academic Year: 2021

Advisor's Signature .....

## ACKNOWLEDGEMENTS

I am grateful to Assistant Professor Palang Bumroongsakulsawat, who gave the advice, counseling, assistance, and motivation for my thesis from the start of the first until the final semester. Besides, I am appreciative to Assistant Professor Apinun Soottitantawat, as the chairman, Assistant Professor Rungthiwa Methaapanon, and Dr. Pongkarn Chakthranont for their helpful advice and invaluable comment.

Moreover, I impress all my friends for giving me help and many valuable suggestions. Furthermore, I am thankful to the best partners, Momay and Tangkwa for their support in all things. Finally, I am also thankful to Chulalongkorn University and the technicians in the laboratory of the Center of Excellence on Catalysis and Catalytic Reaction Engineering (CECC), who provided the assistance.

Pakawat Sengchim

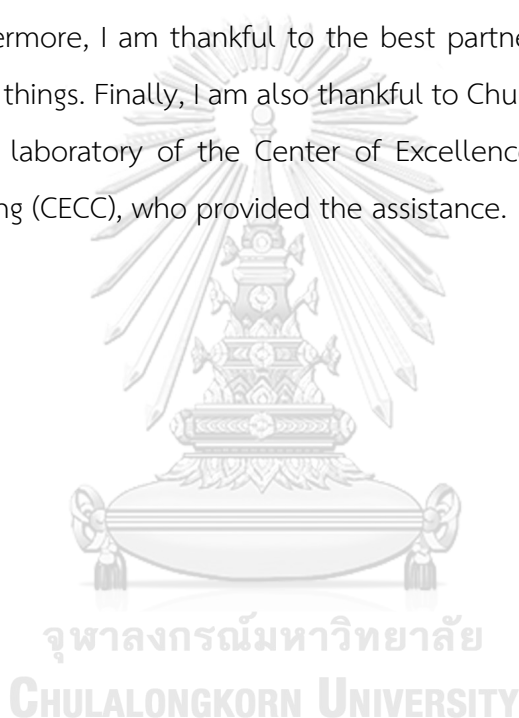


## TABLE OF CONTENTS

	Page
ABSTRACT (THAI) .....	iii
ABSTRACT (ENGLISH) .....	iv
ACKNOWLEDGEMENTS .....	v
TABLE OF CONTENTS .....	vi
LIST OF TABLES .....	viii
LIST OF FIGURES.....	ix
CHAPTER 1 INTRODUCTION .....	1
1.1 Background .....	1
1.2 Objective .....	3
1.3 Scope of Study .....	3
1.4 Expected Benefits.....	3
1.5 Action Plan.....	4
CHAPTER 2 THEORY AND LITERATURE REVIEWS.....	5
2.1. Electrochemical CO <sub>2</sub> reduction reaction .....	5
2.2. Faradaic Efficiency.....	9
2.3 CO <sub>2</sub> in aqueous solution.....	10
2.4. Electrochemical of high pressurized CO <sub>2</sub> .....	10
2.5. Electrodeposition of Zn catalysts .....	15
CHAPTER 3 METHODOLOGY .....	19
3.1 Reactor Design.....	19
3.2 Experimental.....	20



3.2.1. Fabrication of Zn-deposit graphite felt as cathode .....	20
3.2.2. Electrochemical CO <sub>2</sub> reduction.....	21
3.3 Characterization and Product Analysis.....	22
3.3.1. Characterization .....	22
3.3.2. Product analysis.....	22
CHAPTER 4 RESULTS AND DISCUSSION.....	23
4.1 CO <sub>2</sub> reduction reaction .....	25
4.1.1 Voltage effect .....	26
4.1.2 Pressure effect.....	28
4.1.3 CO <sub>2</sub> flow rate effect .....	31
4.2 Blank Test.....	34
CHAPTER 5 CONCLUSION AND SUGGESTIONS.....	35
5.1 Conclusions.....	35
5.2 Suggestions .....	36
REFERENCES.....	37
VITA .....	42

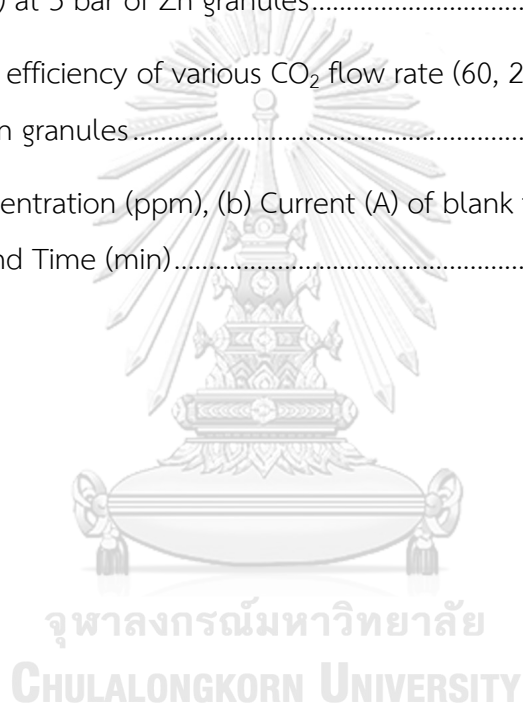
## LIST OF TABLES

	Page
Table 1 Half-cell reaction pathways at cathode and anode in electrochemical CO <sub>2</sub> reduction [9-12].....	6
Table 2 Effect of pressure on the product distribution of different metal electrodes in an electrochemical CO <sub>2</sub> RR process [22] .....	11
Table 3 Summary of CO <sub>2</sub> RR to CO of Zn catalyst.....	16
Table 4 Summary of electrochemical CO <sub>2</sub> RR in tubular fixed-bed reactor of Zn granules .....	25
Table 5 Summary of electrochemical CO <sub>2</sub> RR in tubular fixed-bed reactor of Zn deposited on graphite felt.....	25

## LIST OF FIGURES

	Page
Fig. 1 An outline of electrocatalysts for CO <sub>2</sub> reduction [9].....	8
Fig. 2 Mechanism of electrochemical CO <sub>2</sub> RR for produce CO <sub>2</sub> to CO [19].....	9
Fig. 3 Effect of the pressure of CO <sub>2</sub> on the current efficiency of CO at 12 mA/cm <sup>2</sup> [6]. .....	12
Fig. 4 Effect of pressure on CO <sub>2</sub> RR at 300 mA/cm <sup>2</sup> at various pressures and KOH concentrations [23].....	13
Fig. 5 Faradaic efficiencies of CO obtained at 45 °C [24].....	14
Fig. 6 Impact of pressure on faradaic efficiency of CO [18].....	15
Fig. 7 (a) CO faradaic efficiency for P-Zn and Zn foil and (b) Products distribution of P- Zn in an H-cell reactor [17].....	17
Fig. 8 Faradaic of CO at various constant potentials ranging from -0.6 to -1.1 V [28].	18
Fig. 9 FEs of CO, H <sub>2</sub> , and syngas and CO/H <sub>2</sub> ratios for CO <sub>2</sub> RR on Zn catalysts in CO <sub>2</sub> - saturated 0.1 M KHCO <sub>3</sub> at 40 °C with different potentials [7].....	19
Fig. 10 Electrochemical CO <sub>2</sub> RR cell configuration.....	20
Fig. 11 Schematic of Fabrication of Zn-deposited on graphite felt as cathode.....	21
Fig. 12 Schematic of Electrochemical of high pressurized CO <sub>2</sub> .....	22
Fig. 13 SEM analysis of (a) Graphite felt , (b, c) Zn deposited on graphite felt, and (d) Zn granules.....	24
Fig. 14 (a) CO concentration (ppm), (b) current and Time (min) at 3 bar and CO <sub>2</sub> flow rate 60 ml min <sup>-1</sup> of Zn granules and Zn deposited. ....	28
Fig. 15 CO faradaic efficiency (%) and voltage (5-8 V) at 3 bar and CO <sub>2</sub> flow rate 60 ml min <sup>-1</sup> of (a) Zn granules, (b) Zn deposited on graphite felt. ....	28

Fig. 16 (a) CO concentration (ppm), (b) Current (A) and various pressure (bar) at 8V and CO <sub>2</sub> flow rate 60 ml min <sup>-1</sup> of Zn granules.....	30
Fig. 17 CO faradaic efficiency (%) and various pressure (bar) at 8V and CO <sub>2</sub> flow rate 60 ml min <sup>-1</sup> of Zn granules and Zn deposited.....	30
Fig. 18 (a) CO faradaic efficiency (%), (b) Current and voltage (5-8 V) at 1.5, 3, 8, 10 bar and CO <sub>2</sub> flow rate 60 ml min <sup>-1</sup> of Zn granules.....	31
Fig. 19 (a) CO concentration, (b) Current of various CO <sub>2</sub> flow rate (60, 200 ml min <sup>-1</sup> ) and Voltage (5-8 V) at 3 bar of Zn granules.....	33
Fig. 20 CO faradaic efficiency of various CO <sub>2</sub> flow rate (60, 200 ml min <sup>-1</sup> ) and Time (min) at 3 bar of Zn granules.....	34
Fig. 21 (a) CO concentration (ppm), (b) Current (A) of blank test comparing at 3 bar, 5-8 V, 60 ml min <sup>-1</sup> and Time (min).....	35



# CHAPTER 1

## INTRODUCTION

### 1.1 Background

Nowadays, the concentration of greenhouse gases in the atmosphere is increasing. The main part is carbon dioxide ( $\text{CO}_2$ ), which is strongly linked to global warming and climate change issues. As a potential solution to this challenge,  $\text{CO}_2$  may be converted into valuable products via a carbon dioxide reduction reaction ( $\text{CO}_2\text{RR}$ ) [1].  $\text{CO}_2\text{RR}$  has been proposed as a promising method to combat rising carbon dioxide levels by converting  $\text{CO}_2$  into renewable fuels or valuable chemicals. There are several other methods in  $\text{CO}_2$  utilization, namely thermal catalysis, photochemical reduction, photoelectrochemical reduction, and enzymatic  $\text{CO}_2$  conversion [1, 2]. In comparison with these methods, electrochemical  $\text{CO}_2\text{RR}$  is considered as one of the most useful techniques for the decarbonization process which utilizes clean energy sources and carry out at room temperature. Moreover, electrochemical  $\text{CO}_2\text{RR}$  can be obtained high CO selectivity [1, 3]. CO is an essential product because it is mainly used as a feedstock for the Fischer–Tropsch synthesis, methanol production, and pharmaceutical industry [4].

Generally, Electrochemical  $\text{CO}_2\text{RR}$  is challenging because the low solubility of  $\text{CO}_2$  in aqueous electrolytes at ambient conditions hinders mass transfer of  $\text{CO}_2$  [5]. An interesting strategy to reduce mass transfer limitation is the utilization of gas diffusion electrodes (GDE), and the process carried out at high pressure [6]. Zn catalysts are known to selectivity lead to the product of CO [7]. There are 2 main reactions,  $\text{CO}_2\text{RR}$  at the cathode and oxygen evolution reaction (OER) at the anode. The hydrogen

evolution reaction (HER) is competing with CO at the cathode. These reactions are presented in Eqs. (1)-(6).

#### Cathode reaction (CO<sub>2</sub>RR)



#### Anode reaction (OER)



#### Overall reaction



In this study, a novel scalable electrochemical tubular fixed-bed reactor is developed for gas-phase CO<sub>2</sub> reduction to CO. It features only a single chamber; cathode and anode products are mixed as the reaction gas mixture flows along the reactor. Even though the generated mixture of CO and O<sub>2</sub> presents risk of explosion, this can be avoided by operating outside the flammability limits. For example, flue gas from an incinerator, which contains ca. 5 % CO<sub>2</sub> diluted in mostly N<sub>2</sub>, may be suitable for this reactor. The reactor is made from stainless steel and reactor lining is 3D printed. Saturated CO<sub>2</sub> gas was fed through a porous cathode that consists of Zn catalyst deposited on a carbon support. The effects of CO<sub>2</sub> flow rates, pressure, and applied cell voltages on CO production rates and faradaic yields are studied.

## 1.2 Objective

To study the behavior of the novel electrochemical tubular fixed-bed reactor for electrochemical reduction of  $\text{CO}_2$  to  $\text{CO}$ .

## 1.3 Scope of Study

1.3.1. Pressure applied to the reactor (1-10 bar)

1.3.2. Catalyst is Zinc granules and Zinc deposited on graphite felt

1.3.3. Reaction Conditions were applied voltage (5-8 V),  $\text{CO}_2$  flow rate (60, 200 mL/min), and water is continuously trickled through the bed at 1 mL/min

1.3.4. anion exchange resin beads are used as the electrolyte in the cell.

## 1.4 Expected Benefits

1.4.1. To overcome the main hurdle of the  $\text{CO}_2$  electrochemical conversion in aqueous solution, its low solubility, and to achieve good faradaic efficiency in  $\text{CO}$ .

1.4.2. To explore conditions for scale-up.

จุฬาลงกรณ์มหาวิทยาลัย  
CHULALONGKORN UNIVERSITY

จุฬาลงกรณ์มหาวิทยาลัย  
CHULALONGKORN UNIVERSITY



## CHAPTER 2

### THEORY AND LITERATURE REVIEWS

#### 2.1. Electrochemical CO<sub>2</sub> reduction reaction

Electrochemical CO<sub>2</sub>RR is considered as one of the most useful techniques for the decarbonization process into fuel and chemical products such as CO, CH<sub>4</sub>, HCOOH, and some other products [1, 8]. The electrochemical CO<sub>2</sub>RR occurs at the interface of electrode/electrolyte, which involves three main steps: (i) absorption of the CO<sub>2</sub> on the surface of the catalysts; (ii) transfer of at least two protons and electrons to break one of the oxygen-carbon bonds forming a water molecule in the case of CO or subsequent further protonation; (iii) desorption of the final products from the electrode surface [1, 9]. However, CO<sub>2</sub>RR occurs to need a large negative potential and the E<sub>0</sub> value of hydrogen evolution reaction (HER) derived from hydrolysis of water is relatively positive compared to other C1 products. Then, HER becomes the main competitive reaction of CO<sub>2</sub>RR [9]. Due to this, the CO<sub>2</sub>RR for converting CO<sub>2</sub> into CO, the reaction  $\text{CO}_2(\text{g}) \rightarrow \text{CO}(\text{g}) + \frac{1}{2} \text{O}_2(\text{g})$  has an E<sup>0</sup> value of -1.334 V vs SHE, indicating that it is a non-spontaneous reaction. As a result, this cell requires a voltage greater than the equilibrium electrode potential same as the electrolytic cell. When a cell receives an electrical current from an applied voltage, the electron can transfer from the anode to the cathode, provided that the electron transfers in the system according to the Faraday's law because the electric current that flows through an electrochemical cell is related to the moles of electrons and subsequently occur the CO<sub>2</sub>RR.

The cell of electrochemical CO<sub>2</sub>RR consists of cathode and anode in which CO<sub>2</sub> was continuously fed and applied voltage. At the cathode, there was a CO<sub>2</sub>RR and HER

and at the anode, there was an oxygen evolution reaction (OER) from water is oxidized to molecular oxygen [9, 10]. According to the thermodynamic theory, the minimum potential required for a CO<sub>2</sub>RR is the half-cell standard potential described by  $E^0 = -\Delta G^0/nF$ , where  $-\Delta G^0$  is the Gibbs free energy at 1 atm and 298 K,  $n$  is the number of moles of electrons transferred in the half-cell reaction, and  $F$  is faraday constant (96485 C/mol) [11]. For conversion of CO<sub>2</sub> to CO, the half-cell reaction  $\text{CO}_2(\text{g}) + 2\text{H}^+(\text{aq}) + 2\text{e}^- \rightarrow \text{CO}(\text{g}) + \text{H}_2\text{O}(\text{l})$  with  $\Delta G^0 = 20.09 \text{ kJ/mol}$  has  $E^0 = -0.104 \text{ V}$  vs SHE. Other half-cell standard potentials are shown in Table. 1.

**Table 1** Half-cell reaction pathways at cathode and anode in electrochemical CO<sub>2</sub> reduction [9-12]

Electrode	Half-Electrochemical Reactions	$E_0$ (V vs SHE)
Cathode reaction (CO <sub>2</sub> RR)	$\text{CO}_2 + 2\text{H}^+ + 2\text{e}^- \rightarrow \text{CO} + \text{H}_2\text{O}$	-0.104
	$\text{CO}_2 + 2\text{H}^+ + 2\text{e}^- \rightarrow \text{HCOOH}$	-0.250
	$\text{CO}_2 + 6\text{H}^+ + 6\text{e}^- \rightarrow \text{CH}_3\text{OH} + \text{H}_2\text{O}$	+0.016
	$\text{CO}_2 + 8\text{H}^+ + 8\text{e}^- \rightarrow \text{CH}_4 + 2\text{H}_2\text{O}$	+0.169
	$2\text{CO}_2 + 12\text{H}^+ + 12\text{e}^- \rightarrow \text{C}_2\text{H}_4 + 4\text{H}_2\text{O}$	+0.064
(HER)	$2\text{H}^+ + 2\text{e}^- \rightarrow \text{H}_2$	0.000
Anode reaction (OER)	$2\text{H}_2\text{O} \rightarrow \text{O}_2 + 4\text{H}^+ + 4\text{e}^-$	+1.230

However, the applied voltage affects to consumes CO<sub>2</sub> concentration at the electrode surface, the overall reaction rate can be limited by the rates of CO<sub>2</sub> transfer.

Moreover, according to the Nernst equation, the change in concentration affects the equilibrium electrode potential and this effect can be approximated by the concentration overpotential as the equation (6). Thus, the electrochemical cell improves the minimum energy requirements for CO<sub>2</sub>RR [11, 13] which the Nernst equation gives the relationship between the equilibrium electrode potential and the concentration or partial pressure. The Nernst equation for conversion CO<sub>2</sub> to CO as shown in equation (6) [14].

$$E^0 = \frac{\Delta G_f}{nF} - \frac{RT}{nF} \ln \frac{p_{CO_2}}{p_{CO} \sqrt{p_{O_2}}} \quad (6)$$

Where  $\Delta G_f$  is the Gibbs free energy of formation, R is the gas constant, T is the absolute temperature, n is the moles of electrons transferred in the reaction, F is Faraday's constant,  $p_{CO_2}$  is the partial pressure of CO<sub>2</sub>,  $p_{CO}$  is the partial pressure of CO, and  $p_{O_2}$  is the partial pressure of O<sub>2</sub>.

Furthermore, the difference between the electrode potential and the equilibrium electrode potential is referred to the reaction rate or the electron transfer rate. The kinetics of the electrochemical cell depends on the electrode potential and the equilibrium electrode potential. According to the Butler-Volmer equation as equation (7), increasing the electrode potential affects the electrical current with the exponential relationship [15]. Suppose the electrical current is increased following the cell voltage. It means the electron transfer rate in the electrochemical cell same increased.

$$j = j_0 \{ \exp[-\alpha F \eta / RT] - \exp[(1 - \alpha) F \eta / RT] \} \quad (7)$$

Where j is the electrode current density,  $j_0$  is the exchange current density,  $\alpha$  is the charge transfer coefficient dimensionless, F is Faraday's constant,  $\eta$  is the activation overpotential defined as the difference between the electrode potential

and the equilibrium electrode potential,  $R$  is the gas constant, and  $T$  is the absolute temperature.

A  $\text{CO}_2$  reduction electrocatalyst that can selectively produce desired chemicals while suppressing undesired side reactions is essential to achieve a highly efficient system [6, 16]. Many researchers have investigated the selectivity of products with various metals at the cathode side such as Pd, Ag, Zn, Cu, Sn, Ru, Pt, Ni. Based on the primary  $\text{CO}_2$  reduction product, CO selective metals (e.g., Au, Ag, and Zn), formic acid selective metals (e.g., Sn, In, and Pb), and hydrogen-selective metals (e.g., Fe, Ni, and Pt). [16, 17] as shown in Fig. 1.

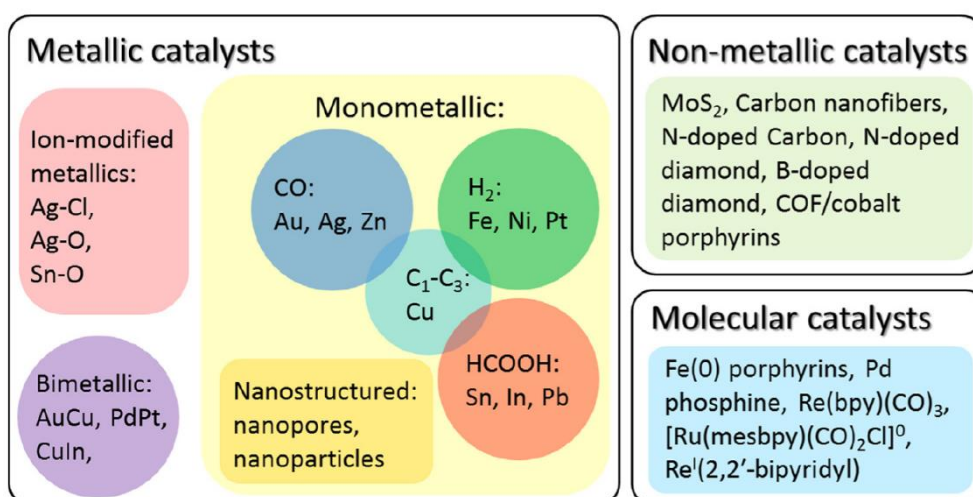


**Fig. 1** An outline of electrocatalysts for  $\text{CO}_2$  reduction [9].

A key challenge of electrochemical  $\text{CO}_2\text{RR}$  is the preparation of catalysts with high activity, selectivity, and stability [5, 16]. Au and Ag are known as the best metal catalysts for conversion  $\text{CO}_2$  to CO with high activity and selectivity. However, it is

difficult to use on a large scale in industrialization, due to the high price and scarce reserve of precious metals [5]. Zn, as an earth-abundant metal, is one of the choices to use as a catalyst to produce CO but with relatively lower activity and CO selectivity than Au and Au. To improve the activity and selectivity of Zn catalysts, many alternatives have been used in the preparation of catalysts such as electrodeposition, anodization, oxide reduction [5, 16, 17].

The mechanism of electrochemical CO<sub>2</sub>RR for produce CO<sub>2</sub> to CO. At the beginning, CO<sub>2</sub> and HCO<sub>3</sub><sup>-</sup> are absorbed on the surface of the electrode. Subsequently, (1) CO<sub>2</sub> is reduced to CO<sub>2</sub><sup>-\*</sup> by one electron from electrochemical process; (2) the CO<sub>2</sub><sup>-\*</sup> is electrochemically reduced to the reaction intermediate of COOH<sup>\*</sup>; (3) the COOH<sup>\*</sup> is reduced with an electron and a proton to CO<sup>\*</sup> that desorbs from Zn to produce the CO gas [18].

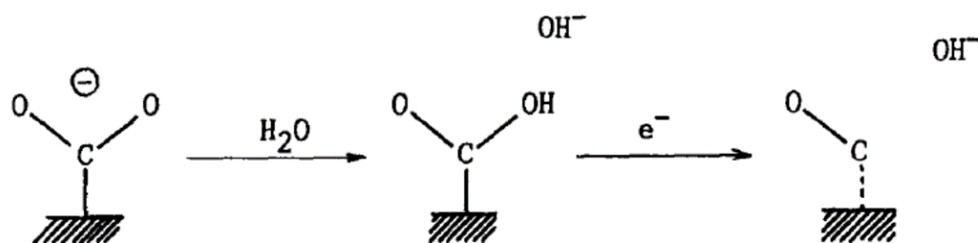


**Fig. 2** Mechanism of electrochemical CO<sub>2</sub>RR for produce CO<sub>2</sub> to CO [19]

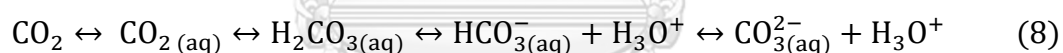
## 2.2. Faradaic Efficiency

Faradaic efficiency (FE) is the parameter of the desired product. It is defined as the electric charge used for the formation of the desired product over the total charge passed between the electrodes. The faradaic efficiency represents the selectivity toward a specific product, thus an improvement on the FE can directly increase the

amount of CO<sub>2</sub> converted to the desired product, reduce product separation cost, and lower the energy penalty of the electrocatalysis.

### 2.3 CO<sub>2</sub> in aqueous solution

Carbon dioxide dissolves in water leading to the formation of CO<sub>2</sub> species such as carbonic acid (H<sub>2</sub>CO<sub>3</sub>), bicarbonate (HCO<sub>3</sub><sup>-</sup>), and carbonate (CO<sub>3</sub><sup>2-</sup>). The equilibrium concentration of these species is a function of the partial pressure of CO<sub>2</sub> and the pH. Under ambient pressure, the solubility of CO<sub>2</sub> in water is about 0.034 mol/L and pH = 3.9. The equation (8) shows that introducing CO<sub>2</sub> in an aqueous solution leads to a complex series of reversible reactions between CO<sub>2</sub> species. In the solution with a pH up to about 6, CO<sub>2</sub> is in the form of a weak carboxylic acid; at pH between 6 and 10.3, HCO<sub>3</sub><sup>-</sup> anions are formed; and at pH above 10.3, HCO<sub>3</sub><sup>-</sup> deprotonates further to CO<sub>3</sub><sup>2-</sup> [11]. Other approaches to increasing the solubility of CO<sub>2</sub> involved the use of high-pressure CO<sub>2</sub> or the use of non-aqueous solvent [20].



### 2.4. Electrochemical of high pressurized CO<sub>2</sub>

In aqueous solvents, the hydrogen evolution reaction (HER) is a competitive reaction with CO<sub>2</sub> reduction reaction (CO<sub>2</sub>RR) because the solubility of CO<sub>2</sub> in water at ambient pressure is low which indicate mass transfer limitations [21]. One strategy to overcome this limitation, the partial pressure of CO<sub>2</sub> in the gas fed into the electrolyzer impacts the rate of CO<sub>2</sub> mass transfer to the electrode surface due CO<sub>2</sub> solvent solubility relationship [11]. However, the high-pressure CO<sub>2</sub>RR requires balancing the

pressure in the anode and cathode chambers to prevent damage to the separator [6, 21].

Hara et al. (1995) [22] studies the electrochemical reduction of CO<sub>2</sub> at high pressure (30 atm) in an aqueous KHCO<sub>3</sub> solution. The electrolysis cell was carried out in a glass cell in a stainless-steel autoclave. The catholyte and anolyte compartments were separated by a Nafion 417 sheet. The electrolyte was deaerated by bubbling CO<sub>2</sub> for 30 min, a known pressure of CO<sub>2</sub> was introduced into the electrolysis cell. In the Zn electrode under a CO<sub>2</sub> pressure of 30 atm at a current density of 163 mA/cm<sup>2</sup>, CO with faradaic efficiencies of 49%.

In Table. 2, summarizes a typical example report of CO<sub>2</sub> pressure (1, 30 atm) on product selectivity over different metal electrodes by Hara et al. For group C, catalysts like Ag, Zn, and Sn, did not report a major shift in the type of CO<sub>2</sub>RR products at higher pressure but the faradaic efficiency towards CO and HCOOH did increase which was affected to increased CO<sub>2</sub> solubility at high pressure [11, 19].

**Table 2** Effect of pressure on the product distribution of different metal electrodes in an electrochemical CO<sub>2</sub>RR process [22]

Group	Cathode catalyst	Effect of pressure	
		Major products at 1 atm	Major products at 30 atm
A	Ti, Nb, Ta, Mo, Mn, Al	H <sub>2</sub>	H <sub>2</sub>
B	Zr, Cr, W, Fe, Rh, Ni, Pd, Pt, Si	H <sub>2</sub>	CO and HCOOH

C	Ag, Au, Zn, In, Sn, Pb, Bi	CO and HCOOH	CO and HCOOH
D	Cu	CH <sub>4</sub> and C <sub>2</sub> H <sub>6</sub>	CO and HCOOH

In the undivided cell. Proietto et al. (2021) [6] studies the electrochemical reduction of pressurized CO<sub>2</sub> to overcome the low solubility of CO<sub>2</sub> in an aqueous solution and achieve good faradaic efficiency. The electrolysis was performed in CO<sub>2</sub> saturated water solution of 0.2 K<sub>2</sub>SO<sub>4</sub> at a silver plate cathode. In this report when the pressure was increased, could lead to a strong enhancement of the CO production. In the same way, the best faradaic efficiency of CO was 67% (30 bar) at 12 mA/cm<sup>2</sup> as shown in Fig. 2. They explain the enhancement of the CO<sub>2</sub> concentration in the bulk is effective to assist the electrocatalytic properties of CO generation.

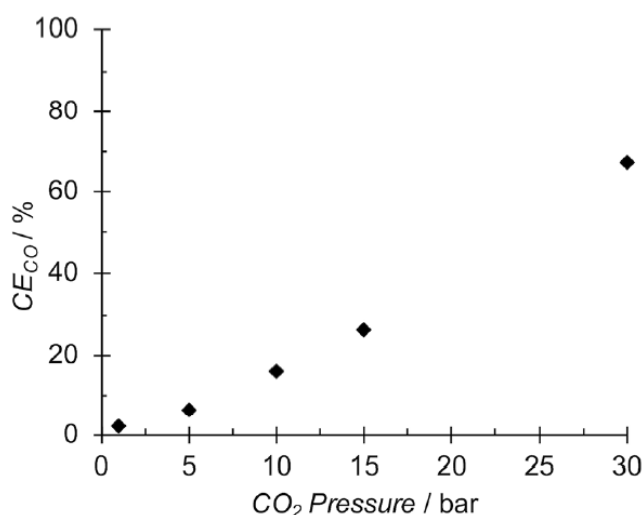


**Fig. 3** Effect of the pressure of CO<sub>2</sub> on the current efficiency of CO at 12 mA/cm<sup>2</sup> [6].

Gabardo et al. (2018) [23] studies to boost the performance of the electrochemical reduction of CO<sub>2</sub> with high alkalinity electrolytes to reduce the



overpotentials needed to generate CO from CO<sub>2</sub> on a silver catalyst. However, these conditions have detrimental effects on product selectivity, increasing the production of formic acid. Therefore, the electrolyzers will need to operate at higher pressure together with high alkalinity electrolytes to achieve the problem. As they hypothesized that an increased concentration of CO<sub>2</sub> on the surface catalyst due to the increase in pressure could lead to increase CO faradaic efficiency and the reaction switching from formic acid to CO and reduce the factors of forming formic acid. From the results in 10 M KOH, the faradaic efficiency of CO increased from 42% (1 atm) to 85% (7 atm) at the current density of 300 mA/cm<sup>2</sup>. However, the faradaic efficiency of formic acid decreased from 38.2% (1 atm) to 12% (7 atm) as shown in Fig. 3.

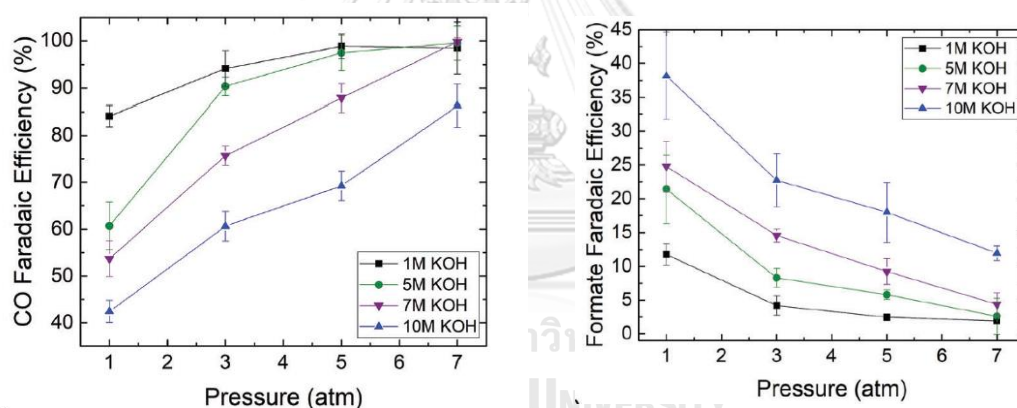


**Fig. 4** Effect of pressure on CO<sub>2</sub>RR at 300 mA/cm<sup>2</sup> at various pressures and KOH concentrations [23].

In the membrane electrode assembly (MEA). Messias et al. (2019) [24] The main objective of this study was to investigate the effect of pressure and the scalability of the process. They have used an inexpensive commercial foil of the common metal zinc as an electrocatalyst. The reactor was operated at 45°C which faradaic efficiency

of CO from 62% at 10 bar to 82% at 30 bar as shown in Fig. 4. The cell potentials of electrolysis carried out in semi-continuous mode were in the range of -3.5 V to -3.9 V vs Ag/Ag<sup>+</sup> QRE. A flow rate of electrolyte at 1 ml/min containing 90 wt% H<sub>2</sub>O and EMIMOTf. The effect of pressure at 30 bar shows a significant influence on CO selectivity and CO productivities. From in Fig. 5 at 10 bar, observe that CO production is higher and presents a maximum at a flow rate of 2.5 ml min<sup>-1</sup>. However, increasing the CO flow rate causes a decrease in the residence time of CO<sub>2</sub> at the electrode surface, influencing the H<sub>2</sub>/CO ratio.

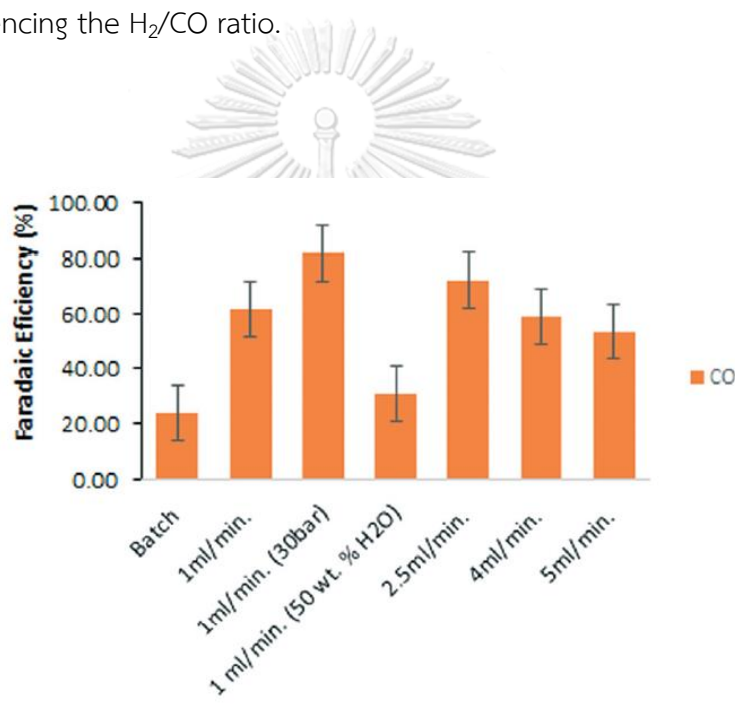


**Fig. 5** Faradaic efficiencies of CO obtained at 45 °C [24]

Meanwhile, Dufek and co-workers (2012) [18]. use Ag-based gas diffusion electrode (Ag GDE) and pressurized CO<sub>2</sub> to address CO<sub>2</sub> reduction is hindered by poor kinetics and limited CO<sub>2</sub> solubility in aqueous solution. The advantage of performing the reduction at high pressure is increasing the pressure increases the solubility of CO<sub>2</sub> according to Henry's law. From the result, they have shown an increase in the faradaic

efficiency for CO generation occurred as the pressure was increased from ambient. At pressures above 15 atm, the faradaic efficiency of CO generation was above 80% at 225 mA/cm<sup>2</sup> and 60 °C. as shown in Fig. 5. In the pressurized cell, the determination of the faradaic efficiency (FE) is complicated by residence time of gases in the system due to the lag time. Thus, elevating flow rate of CO<sub>2</sub> were operated to more effectively sweep product gases from the pressurized electrolysis system and to more readily follow the real-time cell performance.

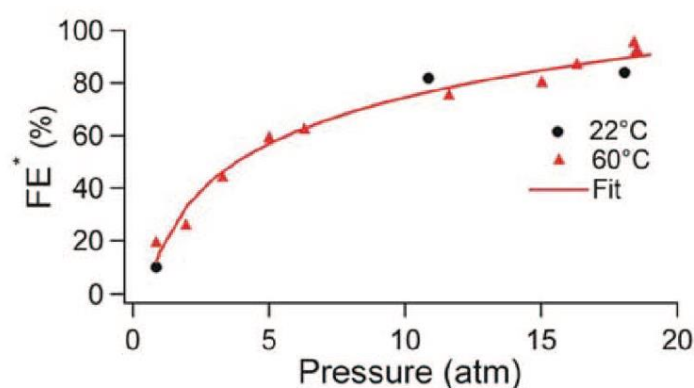


Fig. 6 Impact of pressure on faradaic efficiency of CO [18]

จุฬาลงกรณ์มหาวิทยาลัย  
CHULALONGKORN UNIVERSITY

## 2.5. Electrodeposition of Zn catalysts

The non-noble metal Zn is one of the promising materials because of its abundant reserves and particularly selective production of CO, but the Zn metal reduces CO<sub>2</sub> to CO with low activity and CO selectivity than the noble metal Au and Ag catalyst [17]. To overcome this limitation, efforts have been made to increase the active surface area of a Zn electrocatalyst and allow a much higher CO selectivity [16].

In this report, develop the Zn electrode with the electrodeposition to study the behavior of the tubular reactor. The electrodeposition process is metallic coating onto the porous support (base material), which occurs through the electrochemical reduction of metal ions from an electrolyte. The electrodeposition process consists of the object to be coated or called cathode, electrolyte, anode, and the power supply to make the current flow [25].

**Table 3** Summary of CO<sub>2</sub>RR to CO of Zn catalyst

Researcher	Catalyst	Experimental Condition	CO Faradaic Efficiency
Wen Luo, et al. (2019) [17]	Zn foil	H-cell 0.1 M KHCO <sub>3</sub> -0.95 V vs RHE	50%
	Porous Zn (P-Zn)	H-cell 0.1 M KHCO <sub>3</sub> -0.95 V vs RHE	95%
Lu, Y. et al. (2018) [26]	ED Zn	H-cell 0.5 M KHCO <sub>3</sub> -1.1 V vs RHE	80%
Jonathan Rosen, et al. (2015) [27]	Electrodeposited Zn dendrites	H-cell 0.5 M NaHCO <sub>3</sub> -1.1 V vs RHE	79%
Da Hye Won, et al. (2016) [28]	Hexagonal Zn	H-cell 0.5 M KHCO <sub>3</sub> -0.95 V vs RHE	85.4%
Bin hao Qin, et al. (2018) [7]	Electrodeposited Zn catalyst on Cu foam	H-cell 0.1 M KHCO <sub>3</sub> -0.9 V vs RHE	85%

In an H-cell reactor. Luo et al. (2019) [17] Zn electrocatalyst is synthesized using an electrochemical method to boost the performance of CO<sub>2</sub>RR with electrodeposition method to prepare porous Zn catalyst (P-Zn); that is, the sample deposition of Zn onto the Cu mesh. Interesting this report is the enhanced CO<sub>2</sub> reduction performance of the P-Zn in selectivity compare with Zn foil. From the results, porous Zn catalyst can convert CO<sub>2</sub> to CO at high faradaic efficiency (FE<sub>CO</sub>, ~95%), compared with that of Zn foil (FE<sub>CO</sub>, =50%) as shown in Fig. 7a. Because the Cu mesh used as support played the role in increasing the surface area of P-Zn, and the difference mainly corresponds to lower FEs for H<sub>2</sub> on P-Zn as shown in Fig 7b.

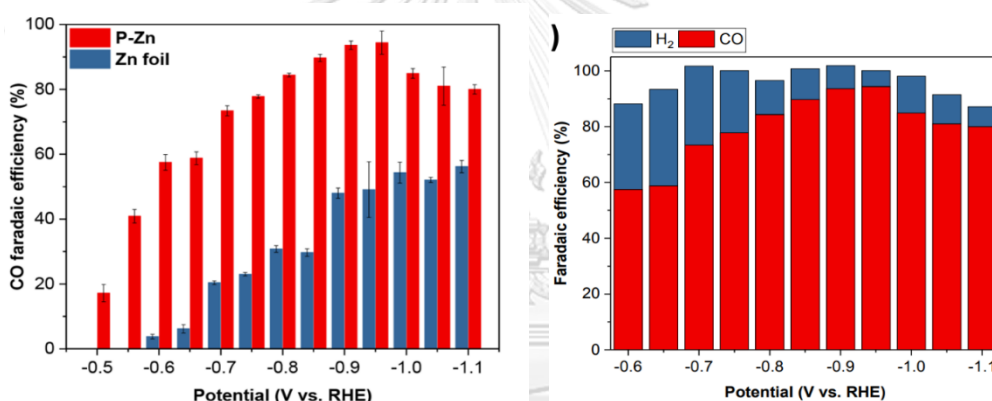


**Fig. 7** (a) CO faradaic efficiency for P-Zn and Zn foil and (b) Products distribution of P-Zn in an H-cell reactor [17].

Luo et al. (2018) [29] studies the ZnO catalysts were synthesized on Zn foil substrates using various preparation methods, containing hydrothermal, spray-coating, and electrodeposition methods. The result found that ZnO catalysts with different morphologies, are nanowires, nanoparticles, and nanoflowers form respectively. Then, the synthesized ZnO catalysts were electrochemically reduced at  $-1.6$  V versus reversible hydrogen electrode (RHE) cause a porous morphology composed of thin hexagonal flakes, which exhibited a higher surface area. The CO<sub>2</sub>RR performances of this catalysts were evaluated in H-cell with CO<sub>2</sub>-saturated 0.1 KHCO<sub>3</sub> as the electrolyte.

It shows that all three catalysts are highly selective towards CO with exceeding 90% FE at moderate overpotentials.

Won et al. (2016) [28] have reported that a hexagonal Zn catalyst that was electrodeposited on a Zn foil had good selectivity of CO. They prepare the hexagonal Zn catalyst by electrodeposition of  $\text{ZnCl}_2$  on Zn foil. The  $\text{CO}_2\text{RR}$  performances were carried out at potential range from -0.6 to -1.1 V (vs RHE) in a  $\text{CO}_2$ -saturated 0.5M  $\text{KHCO}_3$  electrolyte. The highest FE for CO was 85.4% at -0.95 V on the hexagonal Zn, which compared with Zn foil was 25.1% of FE for CO as shown in Fig. 8. In summary, they found that development of the hexagonal Zn catalyst was high selectivity towards CO. In particular, DFT calculations demonstrated that (101) facet is appropriate to CO production due to its lower reduction potential for  $\text{CO}_2$  reduction to CO and higher energy barrier for HER.

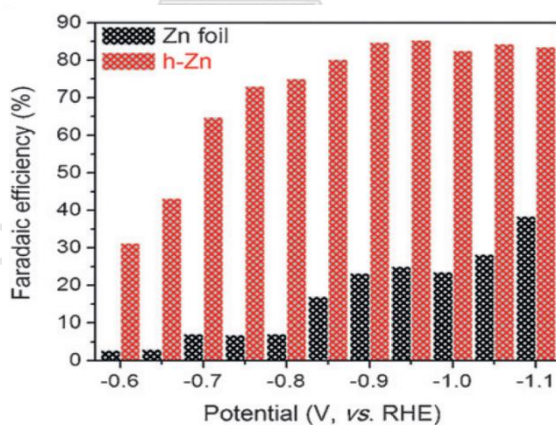


**Fig. 8** Faradaic of CO at various constant potentials ranging from -0.6 to -1.1 V [28].

Qin et al. (2018) [7] studies Zn catalysts have been prepared on electrochemically polished Cu foam by the electrochemical deposition method. For electrocatalytic test for CO<sub>2</sub>RR performances was conducted in an airtight H-cell. the Faradaic efficiency (FE) of CO<sub>2</sub>RR to syngas is greater than 85% at -0.9V vs RHE in aqueous solution.

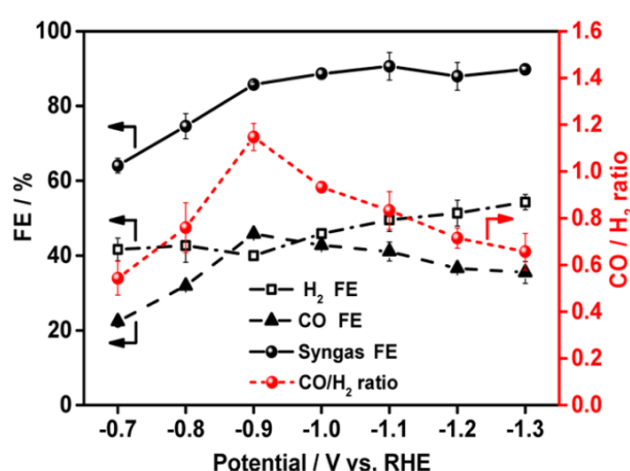


**Fig. 9** FEs of CO, H<sub>2</sub>, and syngas and CO/H<sub>2</sub> ratios for CO<sub>2</sub>RR on Zn catalysts in CO<sub>2</sub>-saturated 0.1 M KHCO<sub>3</sub> at 40 °C with different potentials [7].

## CHAPTER 3

### METHODOLOGY

#### 3.1 Reactor Design

The reactor was made from stainless steel. A reactor lining made by 3D printing was inserted inside the reactor to prevent a short circuit. In Fig. 10 displays the configuration details and the 14 mm cell diameter. There are three main parts in the cell. First, the porous cathode is zinc granules (Sigma-Aldrich) or zinc deposited on graphite felt as a cathode for converting CO<sub>2</sub> to CO that formed at a thickness of 3 mm. Second, the porous solid electrolyte is formed from a 2 mm thick bed of anion-

exchange resin beads (Amberlite IRA402 Chloride form) for ionic conductivity and separation of the electrodes and the anode is platinized titanium mesh (Fuel Cell Store). Finally, graphite felt is used to provide compression for firm electrical contacts between cell components.



**Fig. 10** Electrochemical CO<sub>2</sub>RR cell configuration

### 3.2 Experimental

This work consists of 2 parts: electrochemical conversion of pressurized CO<sub>2</sub> with Zn granule cathodes and Zn graphite felt as cathodes.

#### 3.2.1. Fabrication of Zn-deposit graphite felt as cathode

The cathode was prepared by the electrodeposition method at room temperature and atmospheric pressure. Graphite felt (diameter 14 mm) is used to support which high porosity, high conductivity, and high surface area for disperse gas. A titanium plate was used as the working electrode and the counter electrode in the electrodeposition process, respectively. This process uses 0.1M of ZnSO<sub>4</sub>·7H<sub>2</sub>O (Sigma-



Aldrich) 100 ml as an electrolyte and deposition at a constant 10 mA for 30 mins, as presented in Fig 11.

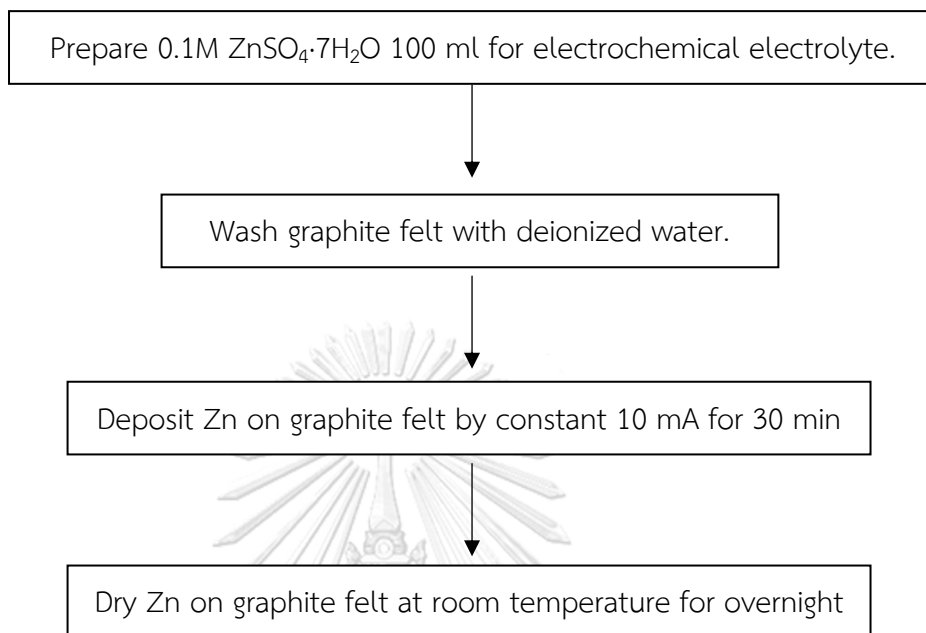


**Fig. 11** Schematic of Fabrication of Zn-deposited on graphite felt as cathode

### 3.2.2. Electrochemical CO<sub>2</sub> reduction

Gas mixtures containing CO<sub>2</sub> are fed continuously to the tubular reactor. The flow rate is controlled by a mass flow controller. Potentiostat galvanostat Autolab PGSTAT101 is used to apply cell voltages for electrochemical CO<sub>2</sub>RR. Water is continuously trickled through the bed at 1 mL/min to sustain the ionic conductivity of the anion-exchange resin bed. Before the test, water was saturated with CO<sub>2</sub> by flowing CO<sub>2</sub> at desired pressure in the water drum overnight, and flowing CO<sub>2</sub> was maintained during the reaction. CO concentration was analyzed by Infrared Gas Analyzer (Model IR200, YOKOGAWA) in real-time as presented in Fig. 12. The effects of Pressure (1.5, 3, 8, and 10 bar), CO<sub>2</sub> flow rates (60 and 200 ml min<sup>-1</sup>), and applied cell voltages (5, 6, 7, and 8 V) will be studied.

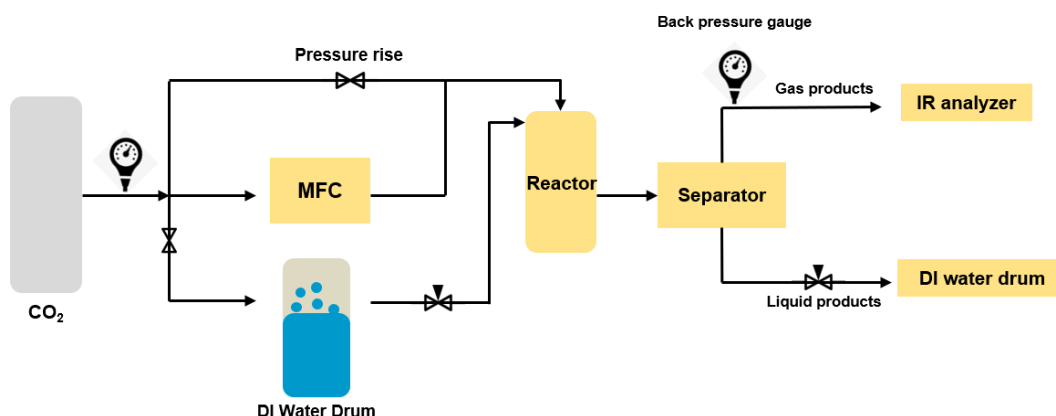


Fig. 12 Schematic of Electrochemical of high pressurized CO<sub>2</sub>

### 3.3 Characterization and Product Analysis

#### 3.3.1. Characterization

3.3.1.1 Scanning electron microscopy with Energy-dispersive X-Ray (SEM-EDX) is a technique that scans the surface with the electron beam. The electrons beam interacts with the sample and a number of signals are produced for detecting a surface of graphite felt. Furthermore, EDX could characterize and measure the elemental composition to confirm that Zn-metal can deposit on graphite felt with the electrodeposition method.

#### 3.3.2. Product analysis

3.3.2.1 The Current from CO<sub>2</sub>RR in an electrochemical tubular reactor could calculate Faradaic efficiency of CO product by Eqs. (9).

$$\begin{aligned} \text{FE\%} &= \frac{\text{Number of moles of electrons required for reducing CO}_2 \text{ to CO}}{\text{Total number of moles of electrons passed}} \\ &= \frac{y \int_0^t C_{\text{CO}} dt \times \text{flowrate} \times F}{\int_0^t I dt} \end{aligned} \quad (9)$$

When

$y$  = Stoichiometric coefficient of electron in Eqs (1), which is 2.

$C_{\text{CO}}$  = Concentration of CO produced at various times

$F$  = Faraday constant

$I$  = Electric current

$t$  = Time

## CHAPTER 4

### RESULTS AND DISCUSSION

The purpose of this work was to study the behavior of the novel electrochemical tubular fixed-bed reactor for electrochemical reduction of CO<sub>2</sub> to CO. The high pressure, applied voltage, and CO<sub>2</sub> flow rate are interesting parameters for preliminary electrochemical CO<sub>2</sub> reduction. In the experimental, the catalyst is Zn granule, and Zn-deposit on graphite felt. Fig. 13 shows the SEM image of Carbon felt, and Zn particles appeared on graphite felt.

The SEM morphology of graphite felt, a smooth carbon fiber with a diameter of 10  $\mu\text{m}$ , is shown in Fig. 13a. After the electrodeposition, Zn was disorderly formed

on the carbon fiber with a diameter of about  $\sim 10\text{ }\mu\text{m}$  in Fig. 13b; however, Zn was only deposited on the surface and not inside the graphite felt, as can be seen from pure carbon fiber inside. Zn morphology on graphite felt is shown in Fig. 3c as hexagonal flakes. In Fig. 13d shows the SEM morphology of Zn granules with spherical, nonspherical shapes and rough surfaces with a diameter of  $\sim 0.5\text{--}1\text{ mm}$ .

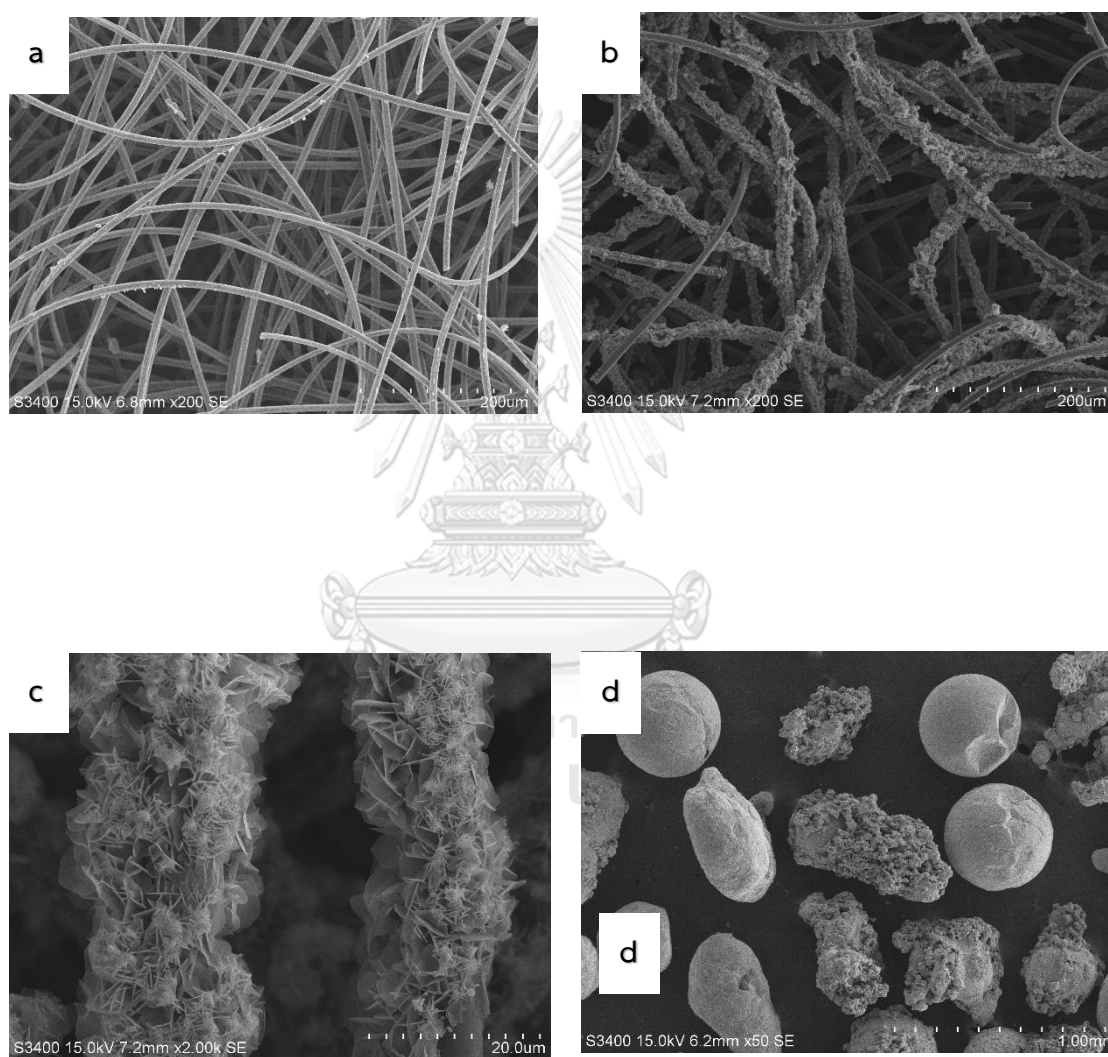


**Fig. 13** SEM analysis of (a) Graphite felt , (b, c) Zn deposited on graphite felt, and (d) Zn granules.

#### 4.1 CO<sub>2</sub> reduction reaction

The summary of electrochemical CO<sub>2</sub>RR experiment both of Zn Granules and Zn deposited on graphite felt as shown in Table 4, 5 respectively.

**Table 4** Summary of electrochemical CO<sub>2</sub>RR in tubular fixed-bed reactor of Zn granules

CO <sub>2</sub> pressure (bar)	Voltage (V)	CO <sub>2</sub> flow rate (ml min <sup>-1</sup> )	%FE <sub>CO</sub>	Current (mA)	CO concentration (ppm)
1.5	8	60	4.72	40.09	245
3	8	60	6.44	91.25	755
8	8	60	10.99	82.07	1225
10	7	60	19.61	50.53	1272
10	8	60	11.42	82.41	1402
3	5	60	15.32	19.83	390
3	6	60	12.28	42.20	665
3	7	60	9.00	67.69	782
3	8	60	6.44	91.25	755
3	5	200	2.95	14.43	54
3	6	200	3.20	13.36	55
3	7	200	4.06	15.41	80
3	8	200	4.55	18.35	107

**Table 5** Summary of electrochemical CO<sub>2</sub>RR in tubular fixed-bed reactor of Zn deposited on graphite felt

CO <sub>2</sub> pressure (bar)	Voltage (V)	CO <sub>2</sub> flow rate (ml min <sup>-1</sup> )	%FE <sub>CO</sub>	Current (mA)	CO concentration (ppm)
3	8	60	3.90	9.73	84
10	8	60	10.24	11.26	148
3	5	200	1.91	6.12	14

3	6	200	1.99	8.78	22
3	7	200	1.84	12.17	29
3	8	200	1.53	12.64	25

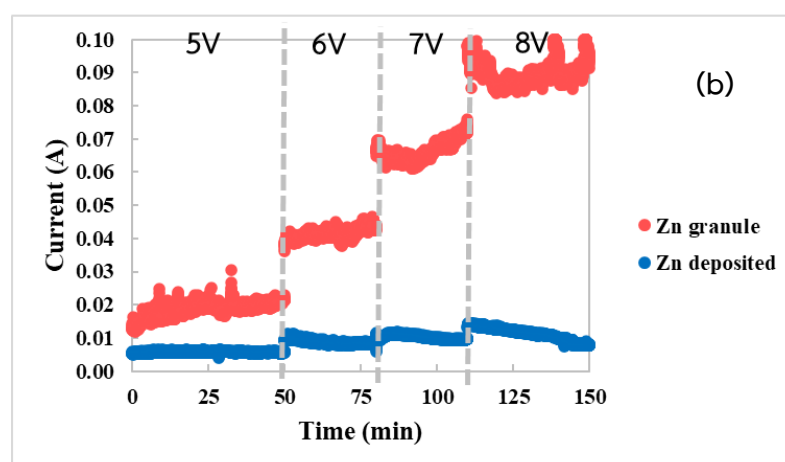
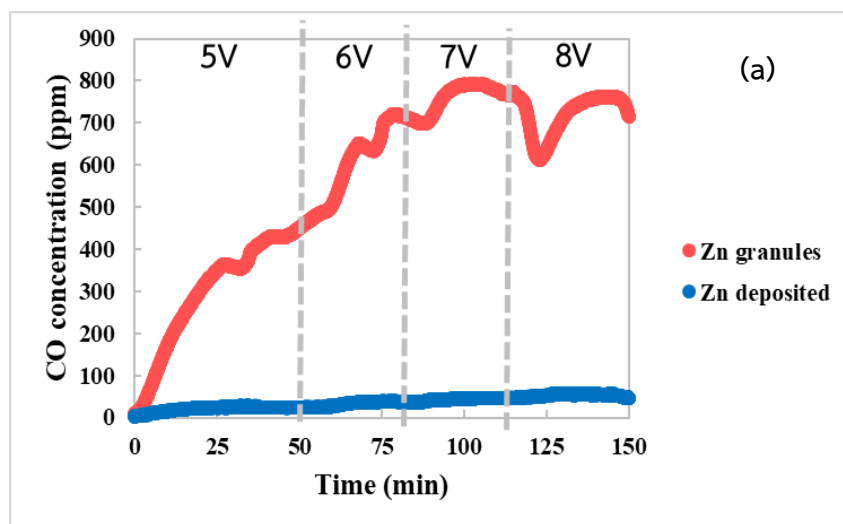
#### 4.1.1 Voltage effect

The voltage condition used in the electrochemical tubular reactor is 5-8 V, CO<sub>2</sub> flow rate and pressure were controlled at 60 ml min<sup>-1</sup> and 3 bar, respectively. As a result, the highest faradaic efficiency, CO concentration, is 15.324% at 5 V and 782 ppm at 7 V.

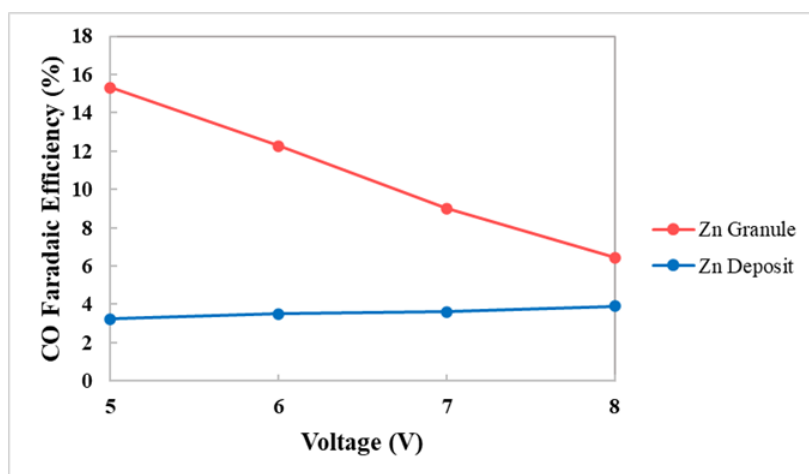
When the applied voltage was elevated in the electrochemical CO<sub>2</sub> reduction reaction, the concentration of CO increased as well, which is consistent with the current that occurred. However, the higher voltage effect CO<sub>2</sub> on the surface of the electrode is quickly consumed, inhibiting the mass transfer limited. [26, 30]. As a result, the CO concentration at 8 V is lower than at 7 V, which occurs from producing more hydrogen evolution reaction (HER) instead of a CO<sub>2</sub> reduction reaction at a high applied voltage, as shown in Fig. 14, and affects decreasing the CO faradaic efficiency as shown in Fig. 15. Additionally, Zn deposited is not inhibiting the mass transfer limited due to the low-rate CO produced.

Fig. 14 and Fig. 15 can explain the Zn electrode both Zn granules and Zn deposited in electrochemical CO<sub>2</sub>RR. From the results, CO concentration and CO faradaic efficiency of Zn granules are higher than Zn deposited which indicates the rate of CO produced in Zn deposited is low. Possibility, (1) Zn deposited to have a low quantity of Zn on graphite felt. The SEM image in fig. 13b, it shows Zn covered the graphite felt surface only, and lower current during the reaction which indicates the low active sites for CO<sub>2</sub> reduction [27, 28] (2) The quantity of Zn on graphite felt is not detectable after the CO<sub>2</sub>RR experiment with Zn deposited for two hours, which influences the rate of CO production and Zn deposited is poor durability. As a

consequence, it can be said that Zn granules perform better than Zn placed at the same thickness of porous cathode.



**Fig. 14** (a) CO concentration (ppm), (b) current and Time (min) at 3 bar and CO<sub>2</sub> flow rate 60 ml min<sup>-1</sup> of Zn granules and Zn deposited.



**Fig. 15** CO faradaic efficiency (%) and voltage (5-8 V) at 3 bar and CO<sub>2</sub> flow rate 60 ml min<sup>-1</sup> of (a) Zn granules, (b) Zn deposited on graphite felt.

#### 4.1.2 Pressure effect

The pressure condition in the electrochemical tubular reactor is 1.5, 3, 8, and 10 bar. During the experiment, the voltage and CO<sub>2</sub> flow rate were controlled at 5-8 V and 60 ml min<sup>-1</sup>, respectively. As shown in Fig. 16, CO concentration increased from 245 ppm at 1.5 bar to 1402 ppm at 10 bar of Zn granules. From the results, when the pressure was increased, the CO concentration was enhanced in Zn granules.

Moreover, the CO faradaic efficiency calculated from experimental data, as shown in Fig. 17, increased the same as the CO concentration in both Zn granules and Zn deposited, which the CO faradaic efficiency of Zn granules increased from 6.44% (3 bar) to 11.42% (10 bar) and Zn deposited is increased from 3.9% (3 bar) to 10.24% (10 bar). For this reason, increasing the CO<sub>2</sub> partial pressure impacts the increased concentration of CO<sub>2</sub> in the electrolyte, which affects the increase in CO<sub>2</sub> surface coverage and reduces the number of protons adsorbed on the catalyst surface to suppress H<sub>2</sub> production, leading to an increase in the CO faradaic efficiency and



decreasing the current density [11, 31] that observes from the current at 10 bar lower than 3 bar in Fig. 16b.

The result can hypothesize that high pressure is enhancing help toward CO faradaic efficiency for the electrochemical tubular fixed-bed reactor. Nevertheless, this result is a preliminary study of the behavior of the system and the major competing side reaction; HER needs to be minimized for an optimal  $\text{CO}_2$  reduction reaction.

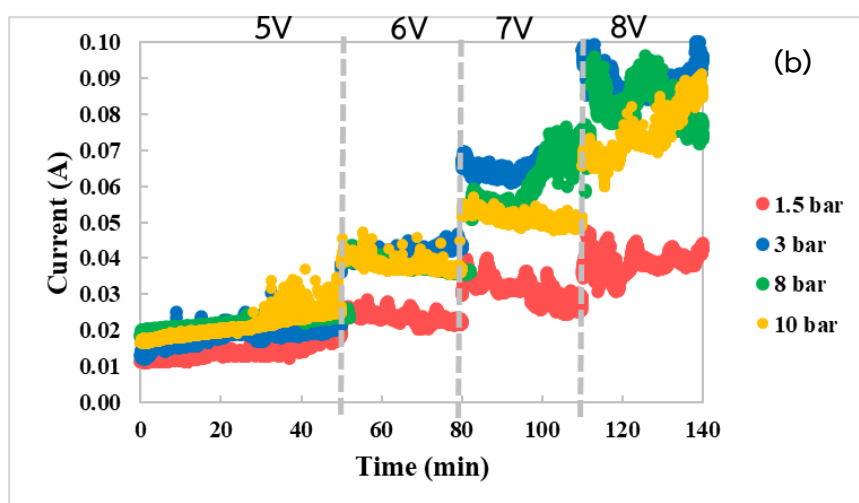
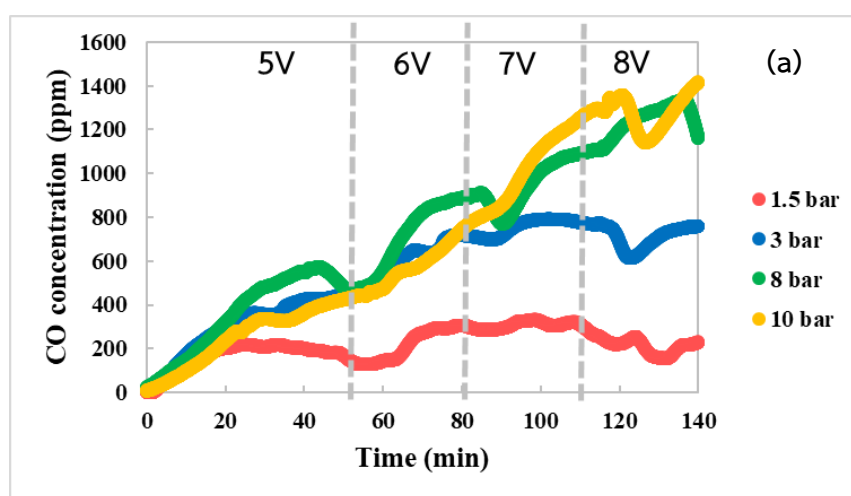


**Fig. 16** (a) CO concentration (ppm), (b) Current (A) and various pressure (bar) at 8V and CO<sub>2</sub> flow rate 60 ml min<sup>-1</sup> of Zn granules.

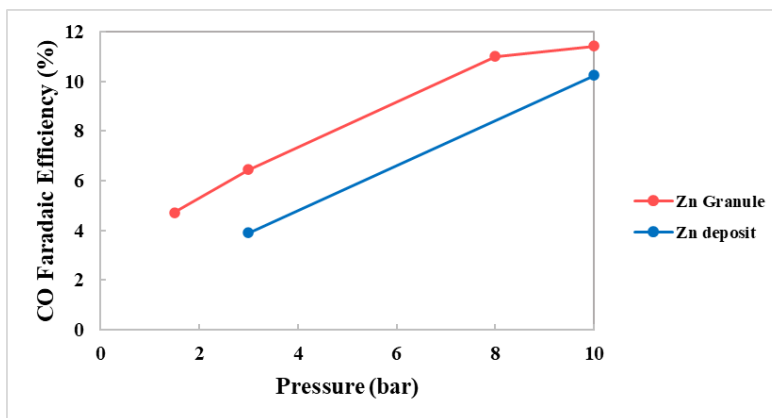


**Fig. 17** CO faradaic efficiency (%) and various pressure (bar) at 8V and CO<sub>2</sub> flow rate 60 ml min<sup>-1</sup> of Zn granules and Zn deposited.

Fig. 18 displays the CO faradaic efficiency and current with applied various voltages from the experiment at each pressure. At 1.5 and 3 bar, the CO faradaic efficiency decreased when the voltage increased due to the over-applied voltage effect, and the highest CO faradaic efficiency was both 5 V. However, at the higher pressure (8 and 10 bar), the highest CO faradaic efficiency shifted from 5 V to 6 V (8 bar) and 7 V (10 bar) as shown in fig. 18a which operates under high-pressure conditions affects the increase of CO<sub>2</sub> on the surface coverage from the pressure effect causes a decrease in mass transfer limited effect of CO<sub>2</sub>, is enough for the CO<sub>2</sub> reduction reaction to produce CO and it can increase the voltage for enhancing the CO faradaic efficiency. The highest CO faradaic efficiency has 19.61% at 10 bar (7 V). Furthermore, the increase of CO<sub>2</sub> on the surface coverage affects the decreasing H<sub>2</sub> formation which causes the total current is decreased. In fig. 18b, the total current for CO<sub>2</sub> reduction at 3 and 8 bar have higher than 10 bar.

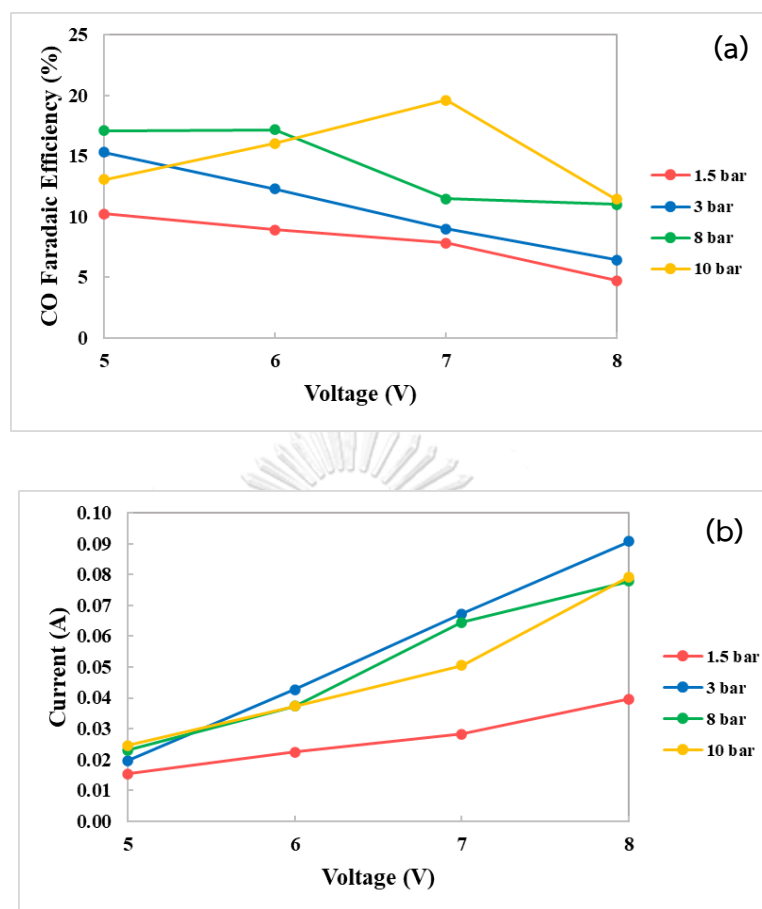


**Fig. 18** (a) CO faradaic efficiency (%), (b) Current and voltage (5-8 V) at 1.5, 3, 8, 10 bar and CO<sub>2</sub> flow rate 60 ml min<sup>-1</sup> of Zn granules.

#### 4.1.3 CO<sub>2</sub> flow rate effect

The CO<sub>2</sub> flow rate condition used in the electrochemical tubular reactor is 60, 200 ml min<sup>-1</sup>. Voltage and pressure were controlled at 5-8 V and 3 bar, respectively. The determination of the CO faradaic efficiency is made difficult by the residence time of product gases that result in a lag in the system. So, increasing the CO<sub>2</sub> flow rate can solve this problem; increasing the CO<sub>2</sub> flow rate can reduce residence time, and the

product gases are quickly flowed into the IR analyzer and can follow the real-time result [18]. However, the higher CO<sub>2</sub> flow rate cause decreasing CO concentration as shown in fig.19, the CO concentration decreased from ~800 ppm (60 ml min<sup>-1</sup>) to ~100 ppm (200 ml min<sup>-1</sup>) because a higher CO<sub>2</sub> flow rate effected to decreases the contact time between catalyst and reactant, leading to a decrease in CO production and CO faradaic efficiency in the system.

As illustrated in fig. 20 of Zn granules at 60 ml min<sup>-1</sup>, the CO<sub>2</sub> reduction process has mass transfers limited at a higher voltage. The higher CO<sub>2</sub> flow rate has no effect on mass transfers at 200 ml min<sup>-1</sup> because the increasing CO<sub>2</sub> flow rate reduces CO production and the amount of CO<sub>2</sub> on the surface is sufficient for the CO<sub>2</sub> reduction.

The CO<sub>2</sub> flow rate effect of Zn deposited on graphite felt at 60-200 ml min<sup>-1</sup>, both CO concentration and current have slightly difference which concludes the flow rate is not effective for the CO concentration and CO faradaic efficiency. So, Using Zn deposited in electrochemical CO<sub>2</sub>RR in a tubular reactor suggests a higher flow rate for reducing lag in the system, which can follow the real-time product gases.

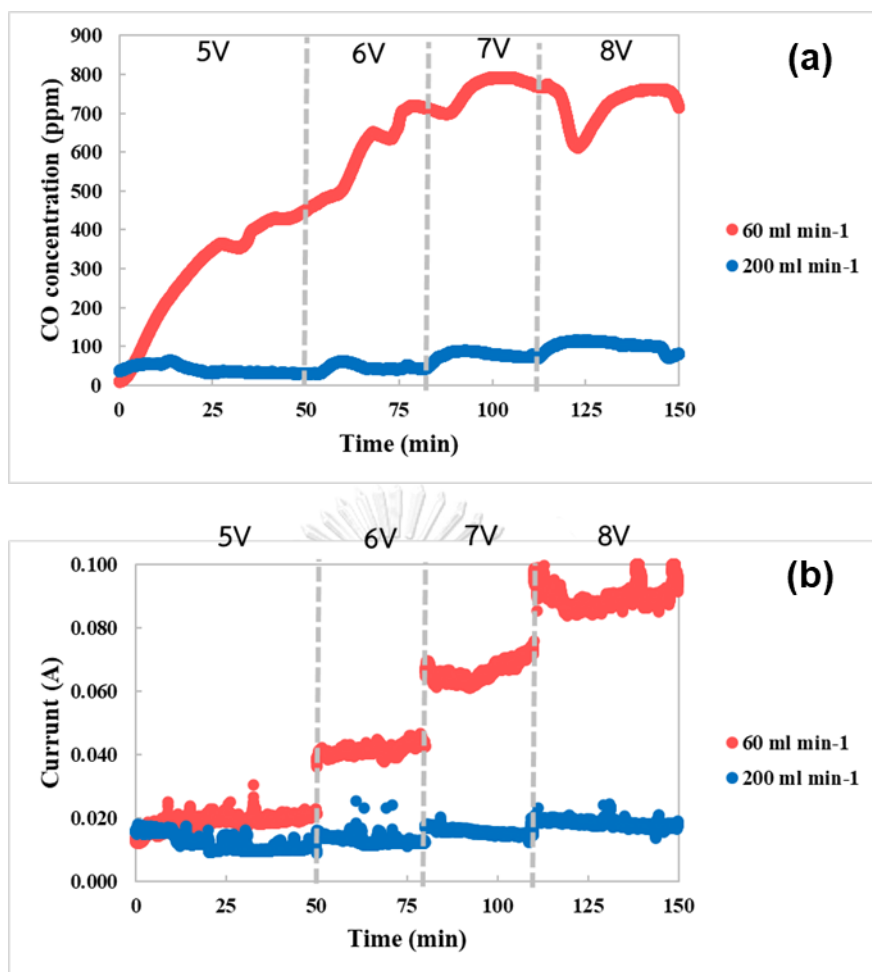
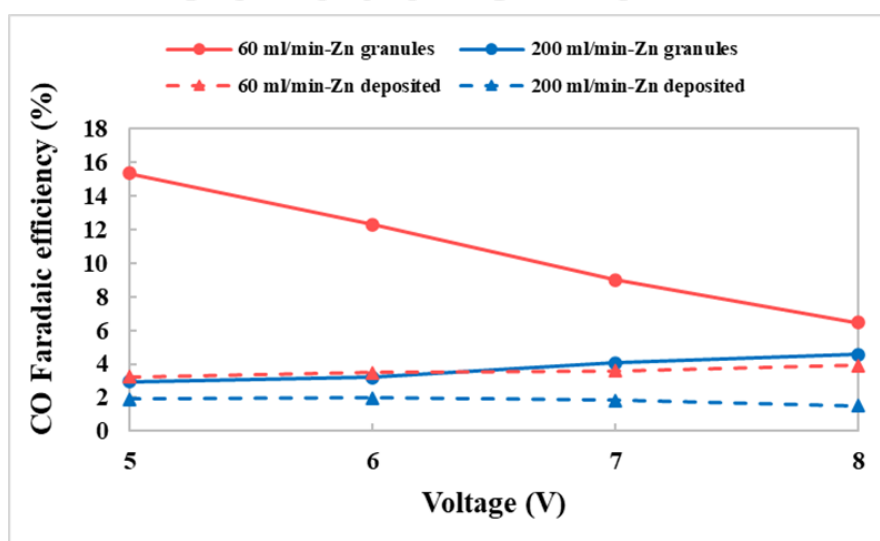


Fig. 19 (a) CO concentration, (b) Current of various CO<sub>2</sub> flow rate (60, 200 ml min<sup>-1</sup>) and Voltage (5-8 V) at 3 bar of Zn granules

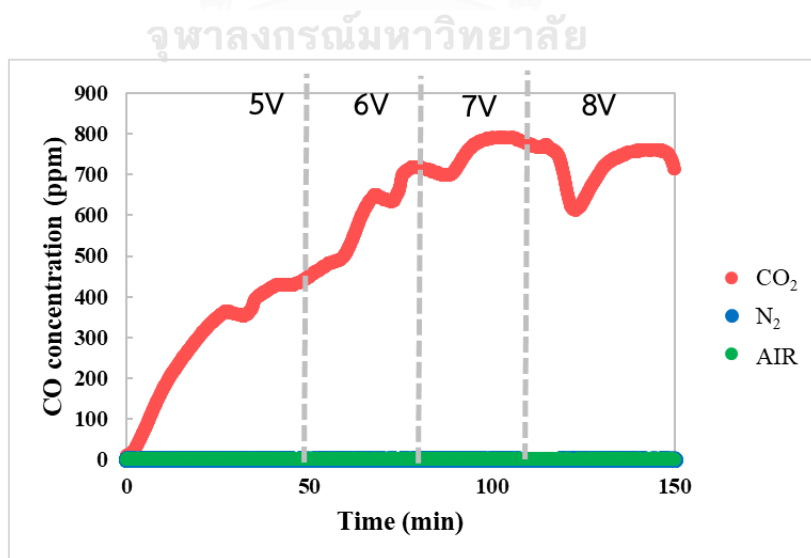


**Fig. 20** CO faradaic efficiency of various CO<sub>2</sub> flow rate (60, 200 ml min<sup>-1</sup>) and Time (min) at 3 bar of Zn granules

#### 4.2 Blank Test

From the results, the behavior of electrochemical CO<sub>2</sub>RR for CO<sub>2</sub> to CO production for confirming CO products is produced with CO<sub>2</sub>RR by feed N<sub>2</sub> replacing the saturated CO<sub>2</sub> gas. The result is shown in Fig. 21a; the amount of CO detected with Infrared Gas Analyzer (IR) was negligible compared with CO<sub>2</sub>RR at 3 bar, 5-8 V, 60 ml min<sup>-1</sup>, resulting indicates the CO production was produced via saturated CO<sub>2</sub>. The current of feed N<sub>2</sub> is lower than the CO<sub>2</sub>RR, which is OER current from only water splitting.

For scale-up in the electrochemical tubular fixed-bed can be a series. Therefore, the possibility of reducing O<sub>2</sub> gas in the next cell decreases the CO faradaic efficiency and CO concentration in the system by feeding Air into the system instead of the saturated CO<sub>2</sub> gas. In Fig. 21b, the current of Air is 1/3 or 1/4 times of CO<sub>2</sub> reduction, indicating the O<sub>2</sub> gas is reduced. Thus, the scale-up the electrochemical tubular fixed-bed must be considering the O<sub>2</sub> gas again.



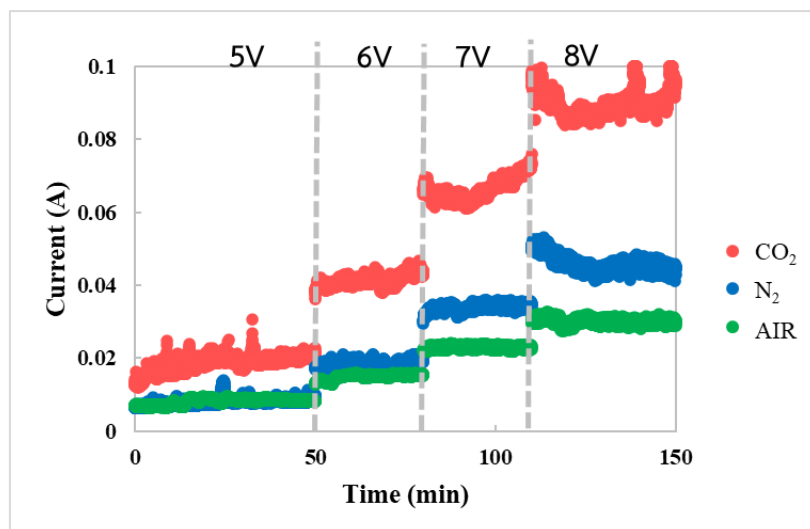
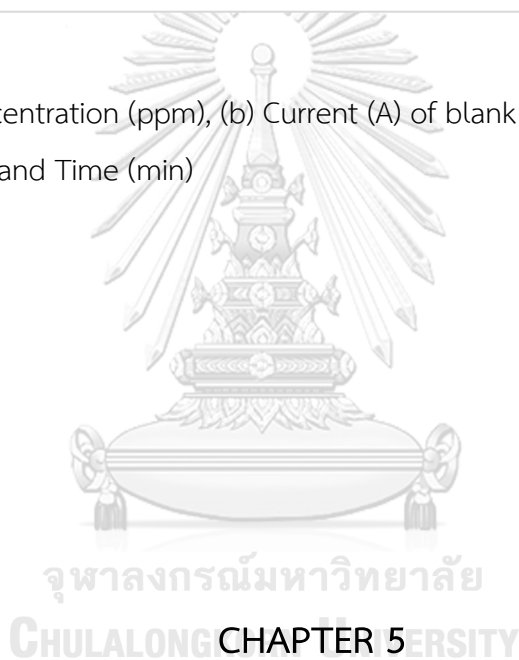


**Fig. 21** (a) CO concentration (ppm), (b) Current (A) of blank test comparing at 3 bar, 5-8 V, 60 ml min<sup>-1</sup> and Time (min)



## CONCLUSION AND SUGGESTIONS

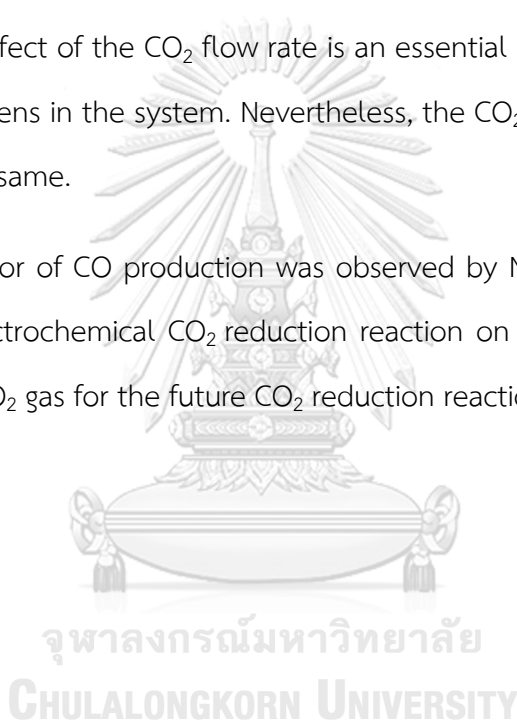
### 5.1 Conclusions

Electrochemical CO<sub>2</sub>RR is usually studied in the liquid phase by electrolyte solution with saturated CO<sub>2</sub> in conventional H-type cells. However, the solubility of CO<sub>2</sub> is low at room temperature and atmospheric pressure leads to mass transfer limitations. So, the development of type cells from H-cell become to tubular is a good

choice for solving this problem because the tubular reactor can carry out at high pressure.

The Electrochemical tubular reactor was studied at high pressure, voltage, and CO<sub>2</sub> flow rate. As soon as increase the pressure, the CO concentration and faradaic efficiency rise. At 10 bar, the highest CO faradaic efficiency of 19.61%. Moreover, at the high-pressure exhibits increase CO faradaic efficiency, CO concentration at higher voltage. The applied voltage suggested for the electrochemical tubular reactor is around 5 V. The effect of the CO<sub>2</sub> flow rate is an essential parameter for reducing the lag time that happens in the system. Nevertheless, the CO<sub>2</sub> flow rate leads to low CO faradaic efficiency same.

The behavior of CO production was observed by N<sub>2</sub> gas, indicate the CO gas occurred with Electrochemical CO<sub>2</sub> reduction reaction on cathode by saturated CO<sub>2</sub> and the behavior O<sub>2</sub> gas for the future CO<sub>2</sub> reduction reaction cell, cannot reduced on the cathode.



## 5.2 Suggestions

- The thickness of the ion-exchange resin bead can be improved to reduce the resistance for the scale-up part of the electrochemical tubular fixed-bed reactor.
- The other product gas and liquid product are produced in the electrochemical CO<sub>2</sub>RR should be detect to analyze and study the behavior of cell.



## REFERENCES

1. Tufa, R.A., et al., *Towards highly efficient electrochemical CO<sub>2</sub> reduction: Cell designs, membranes and electrocatalysts*. Applied Energy, 2020. **277**.
2. Jin, S., et al., *Advances and Challenges for the Electrochemical Reduction of CO<sub>2</sub> to CO: From Fundamentals to Industrialization*. Angew Chem Int Ed Engl, 2021. **60**(38): p. 20627-20648.
3. Lin, R., et al., *Electrochemical Reactors for CO<sub>2</sub> Conversion*. Catalysts, 2020. **10**(5).
4. Jhong, H.-R.M., S. Ma, and P.J.A. Kenis, *Electrochemical conversion of CO<sub>2</sub> to useful chemicals: current status, remaining challenges, and future opportunities*. Current Opinion in Chemical Engineering, 2013. **2**(2): p. 191-199.
5. Wang, G., et al., *Electrocatalysis for CO<sub>2</sub> conversion: from fundamentals to value-added products*. Chem Soc Rev, 2021. **50**(8): p. 4993-5061.
6. Proietto, F., et al., *Electrochemical conversion of pressurized CO<sub>2</sub> at simple silver-based cathodes in undivided cells: study of the effect of pressure and other operative parameters*. Journal of Applied Electrochemistry, 2020. **51**(2): p. 267-282.
7. Qin, B., et al., *Electrochemical Reduction of CO<sub>2</sub> into Tunable Syngas Production by Regulating the Crystal Facets of Earth-Abundant Zn Catalyst*. ACS Appl Mater Interfaces, 2018. **10**(24): p. 20530-20539.
8. Ham, Y.S., et al., *Proton-exchange membrane CO<sub>2</sub> electrolyzer for CO production using Ag catalyst directly electrodeposited onto gas diffusion layer*. Journal of Power Sources, 2019. **437**.
9. Liang, S., et al., *Electrolytic cell design for electrochemical CO<sub>2</sub> reduction*. Journal of CO<sub>2</sub> Utilization, 2020. **35**: p. 90-105.
10. Zhang, X., et al., *Electrocatalytic carbon dioxide reduction: from fundamental principles to catalyst design*. Materials Today Advances, 2020. **7**.

11. Garg, S., et al., *Advances and challenges in electrochemical CO<sub>2</sub> reduction processes: an engineering and design perspective looking beyond new catalyst materials*. Journal of Materials Chemistry A, 2020. **8**(4): p. 1511-1544.
12. Lu, Q. and F. Jiao, *Electrochemical CO<sub>2</sub> reduction: Electrocatalyst, reaction mechanism, and process engineering*. Nano Energy, 2016. **29**: p. 439-456.
13. Gamburg, Y.D., & Zangari, G., *Theory and practice of metal electrodeposition*. 2011.
14. Küngas, R., *Review—Electrochemical CO<sub>2</sub> Reduction for CO Production: Comparison of Low- and High-Temperature Electrolysis Technologies*. Journal of The Electrochemical Society, 2020. **167**(4): p. 044508.
15. Dickinson, E.J.F. and A.J. Wain, *The Butler-Volmer equation in electrochemical theory: Origins, value, and practical application*. Journal of Electroanalytical Chemistry, 2020. **872**: p. 114145.
16. Lee, J., et al., *Electrochemical CO<sub>2</sub> reduction using alkaline membrane electrode assembly on various metal electrodes*. Journal of CO<sub>2</sub> Utilization, 2019. **31**: p. 244-250.
17. Luo, W., et al., *Boosting CO Production in Electrocatalytic CO<sub>2</sub> Reduction on Highly Porous Zn Catalysts*. ACS Catalysis, 2019. **9**(5): p. 3783-3791.
18. Dufek, E.J., et al., *Operation of a Pressurized System for Continuous Reduction of CO<sub>2</sub>*. Journal of The Electrochemical Society, 2012. **159**(9): p. F514-F517.
19. Hori, Y., et al., *Electrocatalytic process of CO selectivity in electrochemical reduction of CO<sub>2</sub> at metal electrodes in aqueous media*. Electrochimica Acta, 1994. **39**(11): p. 1833-1839.
20. Tufa, R.A., et al., *Towards highly efficient electrochemical CO<sub>2</sub> reduction: Cell designs, membranes and electrocatalysts*. Applied Energy, 2020. **277**: p. 115557.
21. Ramdin, M., et al., *High Pressure Electrochemical Reduction of CO<sub>2</sub> to Formic Acid/Formate: A Comparison between Bipolar Membranes and Cation Exchange Membranes*. Industrial & Engineering Chemistry Research, 2019. **58**(5): p. 1834-1847.

22. Kohjiro, H., K. Akihiko, and S. Tadayoshi, *Electrochemical reduction of carbon dioxide under high pressure on various electrodes in an aqueous electrolyte*. J Electronal Chem, 1995: p. 141-147.
23. Gabardo, C.M., et al., *Combined high alkalinity and pressurization enable efficient CO<sub>2</sub> electroreduction to CO*. Energy & Environmental Science, 2018. **11**(9): p. 2531-2539.
24. Messias, S., et al., *Electrochemical production of syngas from CO<sub>2</sub> at pressures up to 30 bar in electrolytes containing ionic liquid*. Reaction Chemistry & Engineering, 2019. **4**(11): p. 1982-1990.
25. Yuliy D. Gamburg, G.Z., *Introduction to electrodeposition: Basic terms and fundamental concepts, Electrodeposition of Zinc and Its Alloys, in Theory and Practice of Metal Electrodeposition*, G.Z. Yuliy D. Gamburg, Editor. 2011, Springer New York, NY. p. 1-25, 284-290.
26. Lu, Y., et al., *Efficient electrocatalytic reduction of CO<sub>2</sub> to CO on an electrodeposited Zn porous network*. Electrochemistry Communications, 2018. **97**: p. 87-90.
27. Rosen, J., et al., *Electrodeposited Zn Dendrites with Enhanced CO Selectivity for Electrocatalytic CO<sub>2</sub> Reduction*. ACS Catalysis, 2015. **5**(8): p. 4586-4591.
28. Won da, H., et al., *Highly Efficient, Selective, and Stable CO<sub>2</sub> Electroreduction on a Hexagonal Zn Catalyst*. Angew Chem Int Ed Engl, 2016. **55**(32): p. 9297-300.
29. Luo, W., et al., *Electrochemical reconstruction of ZnO for selective reduction of CO<sub>2</sub> to CO*. Applied Catalysis B: Environmental, 2020. **273**.
30. Jiang, X., et al., *Electrocatalytic reduction of carbon dioxide over reduced nanoporous zinc oxide*. Electrochemistry Communications, 2016. **68**: p. 67-70.
31. Hori, Y., A. Murata, and Y. Yoshinami, *Adsorption of CO, intermediately formed in electrochemical reduction of CO<sub>2</sub>, at a copper electrode*. Journal of the Chemical Society, Faraday Transactions, 1991. **87**(1): p. 125.



จุฬาลงกรณ์มหาวิทยาลัย  
**CHULALONGKORN UNIVERSITY**



จุฬาลงกรณ์มหาวิทยาลัย  
**CHULALONGKORN UNIVERSITY**

## VITA

NAME	Pakawat Sengchim
DATE OF BIRTH	26 December 1997
PLACE OF BIRTH	Songkhla
INSTITUTIONS ATTENDED	Faculty of engineering, Chemical engineering department Prince of Songkla University Bachelor of Engineering (B.Eng.)
HOME ADDRESS	124, Moo.3, Khlong Hoi Khong, Songkhla, 90230

